James M. Tepper
Neal A. Sharpe
Tibor Z. Koós
Francine Trent

Center for Molecular and Behavioral
Neuroscience and Program in Cellular and
Molecular Biodynamics, Rutgers,
The State University of New Jersey,
Newark, N.J., USA

Postnatal Development of the Rat Neostriatum: Electrophysiological, Light- and Electron-Microscopic Studies

Abstract

The postnatal development of the electrophysiological properties and morphology of rat neostriatum was studied using in vivo and in vitro intracellular recording and biocytin staining and light and electron microscopy. The principal neurons, the medium spiny neurons, were found to undergo a protracted postnatal development of their electrophysiological and morphological characteristics. Most of the intrinsic membrane properties of medium spiny neurons came to resemble those in the adult by the end of the 3rd postnatal week. Synaptic responses and spontaneous activity patterns in medium spiny neurons were dependent on the arrival and functional maturation of excitatory afferents from cortex and thalamus and did not become adult-like until the end of the 1st postnatal month.

Introduction

As the principal input structure of the basal ganglia, the neostriatum plays a critical role in the sensorimotor integrating functions of this subcortical system. The physiological characteristics and morphology of the principal neuron of the neostriatum, the medium spiny neuron, have been well characterized in adult rats [e.g., Bishop et al., 1982; Buchwald et al., 1973; Calabresi et al., 1990a, b; Chang et al., 1982; Chronister et al., 1976; DiFiglia et al., 1976; Kita et al., 1984; Kitai, 1981; Preston et al., 1980; Vandermaelen and Kitai, 1980; Wilson, 1992a, b; Wilson and Groves, 1980, 1981]. Far less is known about the properties of these neurons in neonates or the time course of the postnatal maturation of the neostriatum, particularly in rats.

Neurogenesis in the rat neostriatum begins on embryonic day (ED) 12 with the initial generation of cholinergic interneurons [Phelps et al., 1989]. The medium spiny neurons which are destined to end up in the patch compartment are the next to differentiate, beginning at ED 12, followed at ED 17 by matrix neurons, and the period of active neurogenesis extends at least through ED 22 [Bayer, 1984; Fishell and Van der Kooy, 1987; Van der Kooy and Fishell, 1987]. In both morphological and electrophysiological terms, neostriatal neurons, particularly the medium spiny neurons, undergo a prolonged postnatal maturation that is not complete for several weeks after birth.

Previous light-microscopic studies of intracellularly labeled or Golgi-stained medium spiny neurons have reported that during the early postnatal period (i.e., prior to postnatal day 10 (PD 10) in cats, PD 21 in rats, PD 7 in monkeys, and PD 9 in dogs), neostriatal neurons bear an immature appearance that is characterized by an absence or sparsity of spines and the presence of varicosities on distal dendritic segments [Adinolfi, 1977; Chronister et al., 1976; DiFiglia et al., 1980; Hull et al., 1981; Levine et

J.M. Tepper
Center for Molecular and Behavioral Neuroscience
Rutgers, The State University of New Jersey, University Heights, 197 University Avenue
Newark, NJ 07102 (USA)
Tel. +1 (973) 353 1080, Fax +1 (973) 353 1588, E-Mail tepper@axon.rutgers.edu

al., 1986; Lu and Brown, 1977; Tanaka, 1980; Tepper and Trent, 1993; Trent and Tepper, 1993]. A similar dendritic immaturity has been reported for grafted neostriatal neurons which also possess a reduced density of dendritic spines even after many months of maturation in the host brain [DiFiglia et al., 1988; Walsh et al., 1988; Wilson et al., 1990b; Xu et al., 1992; Zemanick et al., 1987].

In addition, electron-microscopic studies of developing rodent, feline, canine and primate neostriatal neurons have also revealed a prolonged postnatal maturation of synaptic inputs [e.g., Adinolfi, 1977; DiFiglia et al., 1980; Hattori and McGeer, 1973; Lu and Brown, 1977; Sharpe and Tepper, 1998; Tanaka and Alexander, 1978; Tanaka, 1980]. In adults, over 90% of cortical afferents contact the heads of dendritic spines forming asymmetric synapses with the presynaptic bouton containing small round vesicles [Kemp and Powell, 1971a–c]. During the first 2 postnatal weeks in rats the overall density of synapses is relatively low and symmetric synapses make up a greater proportion of total synapses than in the adult [Hattori and McGeer, 1973; Sharpe and Tepper, 1995, 1998]. In rats, the majority of synaptic contacts are formed during the 3rd postnatal week as indicated by a decrease in the extracellular space, an increase in the density of axon terminals, and a more densely packed neuropil [Hattori and McGeer, 1973; Sharpe and Tepper, 1998].

The present studies describe the postnatal development of neostriatal neurons and their afferent connections using in vivo intracellular recording and biocytin staining, visually guided whole cell recording in vitro, and light and electron microscopy. Characterizing the differences in the physiology and morphology of neostriatal neurons among neonates and adults, and the time course of the maturation of these neurons is important not only for determining how the functional organization of the adult neostriatum comes about, but may also have relevance to interpreting the results of physiological and morphological studies of neostriatal grafts and how these differ from the normal intact striatum. In addition, visually guided whole cell patch clamp recording has become a common way to perform in vitro electrophysiological experiments, and the slices used in such experiments are usually taken from very young animals because the visualization and sealing is better than in adults and because the slices survive better. The advent of the wide use of this technique makes it especially important to examine the electrophysiological properties of neonatal neurons to ensure that the results obtained from the whole cell studies are applicable to adult neostriatum.

Methods

In vivo Intracellular Recording and Biocytin Staining

The subjects for these experiments were Sprague-Dawley rat pups ranging in age from PD 6 through PD 49, and adult male Sprague-Dawley rats, where the day of birth is defined as PD 1. Rats were bred at the Institute of Animal Behavior at Rutgers from stock obtained from Charles River. Pups and adults were anesthetized with urethane (1.2–1.5 g/kg, i.p.). When necessary, adults were supplemented with ketamine (20–30 mg/kg, i.m.), and pups were supplemented by inhalation of Metofane. Adults and pups older than 21 days were installed into a stereotaxic frame and prepared for in vivo intracellular recording by conventional means [see Tepper et al., 1987 for details]. Younger neonates were affixed to a modified stereotaxic apparatus by a modification of the method originally described by Nakamura and colleagues [1987]. Briefly, pups were placed on a custom stage designed to hold their head parallel to the stereotaxic frame bars. After removal of the scalp, a small 3-cm stainless steel rod which had short lengths of 3 mm outside diameter (o.d.) stainless steel tubing soldered to the ends was affixed to the top of the skull in the coronal plane approximately 3.5 mm anterior to lambda with cyanoacrylate glue and dental cement. Standard stereotaxic earbars were inserted into the hollow tubes, and the pups' four extremities were affixed to the stage with cyanoacrylate glue. To minimize respiratory artifacts and stabilize the preparation, pups were suspended with a small tail clamp. Body temperature was maintained at $37 \pm 1\,°C$ by a solid state feedback controlled heating pad.

Microelectrodes were pulled from 2.0 mm o.d. capillary tubing, filled with 1 M potassium acetate containing 3% biocytin and possessed in vivo impedances between 75 and 90 MΩ. At the completion of electrophysiological experiments, neurons were intracellularly stained with biocytin by passing 300 ms square wave pulses of 1–3 nA with a 50% duty cycle through the recording electrode for 5–20 min while monitoring the neuron's response through the bridge circuitry of a Neurodata IR-183 preamplifier. Staining was stopped immediately upon deterioration of the recording.

Following a brief survival period (30 min to 2 h), an overdose of urethane was administered, and rats were perfused with 20–50 ml of isotonic saline followed by 50–250 ml of 4% paraformaldehyde-0.2% glutaraldehyde in 0.15 M sodium phosphate buffer, pH 7.4. The brains were removed, left in the same fixative overnight, and sectioned on a Vibratome® at 60 μm and reacted for the presence of biocytin using a Vectastain ABC kit and 3,3′-diaminobenzidine as the chromogen as described by Horikawa and Armstrong [1988].

Intracellularly labeled neurons were located and photographed. Representative cells from each age group were reconstructed from drawings of serial sections using a 60× or 100× oil immersion lens on a Nikon Optiphot® microscope equipped with a drawing tube.

Data were pooled by assigning animals to one of the following age groups: PD 6 to PD 10, PD 11 to PD 15, PD 16 to PD 20, PD 21 to PD 29, PD 30 to PD 40, and adult, and were analyzed with one-way analyses of variance by age group.

In vitro Visualized Whole Cell Recording

Sprague-Dawley rat pups between PD 14 and PD 35 were used. Rats were deeply anesthetized with 80 mg/kg ketamine and 15 mg/kg xylazine and exposed to 95% O_2-5% CO_2 for several minutes. Rats were perfused intracardially with 4 ml of modified, low Ca^{2+}-high Mg^{2+} ice-cold oxygenated rat Ringer's solution (slicing medium) containing (in mM): NaCl 125, KCl 2.5, CaCl$_2$ 0.5, MgCl$_2$ 3.5, NaHCO$_3$

26, NaH$_2$PO$_4$ 1.25, and glucose 8.0, pH 7.3–7.4, saturated with 95% O$_2$-5% CO$_2$. Osmolarity was adjusted to 300 ± 5 mosm. The brain was rapidly removed, and 300–350 μm horizontal sections of the dorsal neostriatum cut on a Campden Instruments Vibroslice® in the same medium. Subsequently, sections were kept at 31–33°C and continuously superfused with normal Ringer's solution at a rate of 10–20 ml/min for 1–2 h. The normal Ringer's solution differed from the slicing medium in that it contained 2.5 mM CaCl$_2$ and 1.5 mM MgCl$_2$.

Single slices were tranferred to a small submerged slice recording chamber (~0.3 ml volume) which was superfused at a rate of 1–2 ml/min with normal Ringer's solution and maintained at 31–33°C. Neostriatal neurons were visualized with infrared differential interference contrast (IR-DIC) using an Olympus BX50 microscope with a 40× long working distance water immersion objective and an IR-sensitive video camera (Dage CCD300).

Whole cell recordings were obtained with patch pipettes pulled from 1.5/1.1 mm o.d./inside diameter borosilicate or 1.5/1.0 mm Corning No. 7052 capillary glass (WPI) on a Narishige PP-83 pipette puller. Pipettes had open tip diameters of 1.5–2.0 μm and impedances of 3–7 MΩ. The intracellular filling solution contained (in mM): 129.4 K-gluconate, 11.1 KCl, 2 MgCl$_2$, 10 HEPES (free acid), 3 Na$_2$ATP, 0.3 GTP, 20 μM EGTA. The pH was adjusted to 7.2–7.3 with KOH.

Electron-Microscopic Studies: Tract Tracing
Adult (older than 8 weeks), PD 21, P14/15 (PD 15) and P9/10 (PD 10) rats were used. For each group, pups were obtained from 3–4 litters. Rats were anesthetized with ketamine (80 mg/kg) and xylazine (15 mg/kg) in 0.9% saline administered intraperitoneally. Glass micropipettes were pulled from 2 mm o.d. capillary tubing on a vertical pipette puller. The tips were broken back to approximately 50 μm under microscopic control and the micropipettes filled with 3–5% biocytin in 1 M potassium acetate. A small burr hole was drilled above the ipsilateral lateral frontal agranular cortex and biocytin was iontophoretically injected (7.5 μA, 7-second pulse, 50% duty cycle, for 15 min in the neonates and for 40 min in adults). Stereotaxic coordinates in adults were from bregma: anterior +2.5, lateral 3.4, ventral 1.75 below the cortical surface. Coordinates were adjusted in neonates to obtain similar injection locations in both adults and neonates and ranged from anterior +2.3 to 2.6, lateral 2.0 to 2.2, ventral 1.8 to 2.3.

Tissue Processing
Four to 24 h postinjection (the older the animal the longer the postinjection time), rats were given an overdose of urethane, perfused with 10–40 ml oxygenated Ringer's followed by 100–400 ml of a 4% paraformaldehyde-0.8% glutaraldehyde solution (pH 7.2) and the brain excised. The brains were blocked and postfixed in the aldehyde fixative solution for at least 24 h. Parasagittal Vibratome sections (30–60 μm) containing neostriatum and the cortical injection site were obtained and processed according to standard protocols previously described [Horikawa and Armstrong, 1988; Sharpe and Tepper, 1998] prior to section embedding between Liquid Release®-coated slides and coverslips.

Analysis
Tissue was initially evaluated at the light-microscopic level. Areas of biocytin labeling in the neostriatum and the injection sites in the cortex were identified and photographed. Areas of interest were resectioned, stained with lead citrate (0.5%) and examined using a Phillips CM10 transmission electron microscope at 80 kV.

The densities of asymmetric and symmetric synapses were determined by analyzing pseudorandomly selected electron micrographs (only micrographs which included at least one synapse were included in the analysis) taken at a magnification of 21,000×. The total number of asymmetric or symmetric synapses in each group was divided by the total area of tissue examined and the resulting density of synapses expressed as the number of synapses/100 μm^2. Group means for the density of synapses were compared by a one-way analysis of variance followed by a post hoc comparison (Fisher's PLSD). All values are reported as mean ± standard error. Significance was declared at p < 0.05 and p values which were less than 0.01 were reported as p < 0.01.

Results

Electrophysiological Observations
In vivo Intracellular Recordings. The electrophysiological properties of medium spiny neurons and their responses to afferent input have been well characterized in vivo and in vitro in adult rats [e.g., Buchwald et al., 1973; Calabresi et al., 1990a,b; Kita et al., 1984; Kitai, 1981; Morris et al., 1979; Vandermaelen and Kitai, 1980; Wilson, 1992a,b; Wilson and Groves, 1981]. The passive membrane properties of these neurons are dominated by a very pronounced, fast inward rectification that results in a relatively low input resistance when the neurons are at rest or are hyperpolarized [see Wilson, 1992a for review]. In contrast, medium spiny neurons from neonatal rats lack inward rectification [Tepper and Trent, 1993; Trent and Tepper, 1991] and most exhibit a fairly linear current-voltage relation as shown in figure 1. The proportion of neurons that exhibited inward rectification increased steadily throughout postnatal development and reached a plateau by the end of the 3rd postnatal week but still had not reached adult levels by the 5th postnatal week, the oldest age at which neonates were examined. The input resistance decreased concomitantly and by PD 21–29 no longer differed significantly from that in adults.

The mean resting membrane potential in neurons recorded in the youngest animals (i.e., PD 6–10) was –45.2 ± 1.9 mV (n = 86), which was significantly less hyperpolarized than that in older neonates and adults (df = 5, 416; F = 11.4; p < 0.01). Over the next 2 weeks, the resting membrane potential became more hyperpolarized (i.e. –62.2 ± 2.2 mV, n = 141 in the PD 21–29 group) when it was no longer different from the value in adults (–61.3 ± 1.9 mV, n = 80).

Approximately 17% of medium spiny neurons in PD 6–10 pups, 25% in PD 11–15 pups and 18% in PD 16–20

Fig. 1. Neonatal neostriatal medium spiny neurons lack inward rectification. **A** Typical membrane responses evoked by intracellular current pulses in a PD 10 pup. Note the linear current-voltage relation. **B** Neuron from a PD 17 pup displays slight inward rectification in both depolarizing and hyperpolarizing directions. Note the early spikes in response to the depolarizing current injections. **C** Adult medium spiny neuron exhibits marked inward rectification and a ramp depolarization in response to depolarizing current injections. Note the long latency to spike discharge. **D** Summary of the postnatal changes in the expression of inward rectification and input resistance. Numbers within parentheses indicate number of neurons per group. Asterisks indicate significantly different from adult group. **A, B** Each trace is the average of 4 sweeps. **C** Composed of single sweeps. Figure modified from Tepper and Trent [1993] with permission.
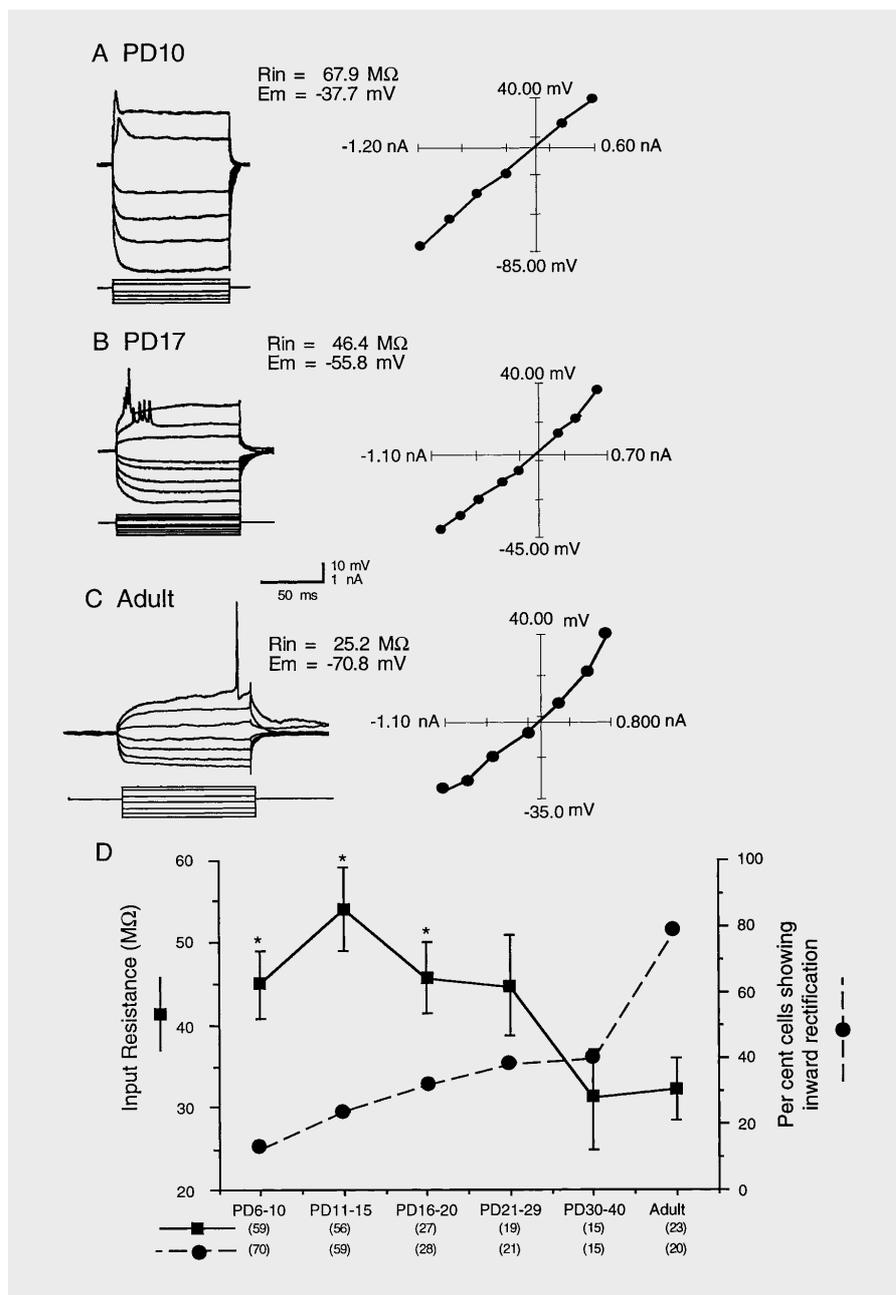
pups exhibited I-V curves dominated by a strong outward rectification [Tepper and Trent, 1993]. This was never observed in pups older than 20 days. In adults, medium spiny neurons fire spontaneously at a low mean rate in an episodic bursty pattern in vivo. The membrane potential of adult spiny neurons in vivo alternates between a hyperpolarized 'down' state, near the potassium equilibrium potential, during which the neurons never fire, and a depolarized 'up' state, during which the neurons may fire [Wilson, 1992b; Wilson and Kawaguchi, 1996]. This bistable behavior has been shown to be due to the interaction of the inward rectifier and a phasic depolarizing input from cortex [Stern et al., 1997; Wilson, 1992b; Wilson and Kawaguchi, 1996]. In neonates the situation is very different, since they do not express the inward rectifier and since the majority of the cortical input has not yet arrived [Hattori and McGeer, 1973; Sharpe and Tepper, 1998]. Spontaneous activity was exceedingly rare during
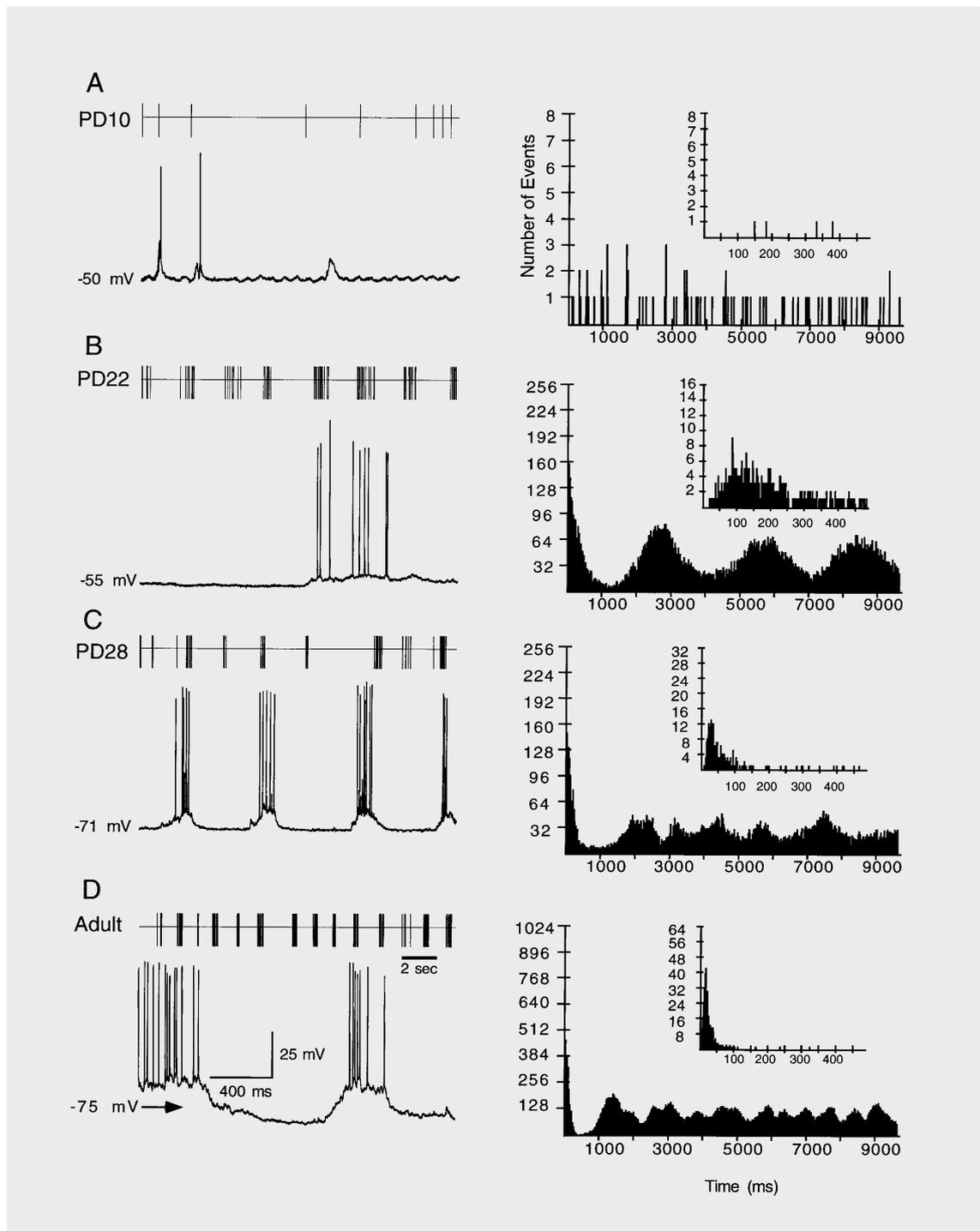
Fig. 2. The rate and complexity of spontaneous activity increase over postnatal development as indicated by spike trains (upper left panels), first order interval histograms (upper right panel insets) and autocorrelograms (lower right panels) constructed from extracellular recordings obtained immediately prior to impalement and digitized traces of subsequent intracellular recordings (lower left panel). **A** Note the sparse spontaneous activity. During the 3rd postnatal week spikes are fired in episodes that occur at regular intervals as indicated by the spike train and autocorrelogram in **B**. **C** By the end of the 4th postnatal week action potentials occur at irregular intervals as indicated by the spike train and intraburst intervals shorten resulting in spontaneous activity that closely resembles that seen in adults (**D**). Bin width = 20 ms for autocorrelograms; bin width for first-order interval histograms = 1 ms. Upper calibration bar applies to all extracellularly recorded spike trains. Lower calibration bar applies to all intracellular records.

the first 2 postnatal weeks, and discrete up and down states were not apparent as illustrated in figure 2A. By the end of the 3rd postnatal week, concomitant with the development of the expression of inward rectification and the arrival of the majority of the corticostriatal inputs, there was an increase in spontaneous activity in the form of rhythmic bursting but the majority of neurons did not yet show clear up and down states (fig. 2B). By the end of the 4th postnatal week, the neurons showed up and down states and fired spontaneously in episodic bursts similar to those seen in the adult (fig. 2C, D).

Although spike threshold remained constant over development, there were changes in some of the other characteristics of action potentials, as summarized in table 1. With the exception of the rate of repolarization which was still significantly slower in the oldest neonates (PD 30–40) than in adults, the properties of action potentials became adult-like by PD 15, at least a week or two before the rate and pattern of spontaneous activity had matured.

In adults, medium spiny neurons respond to stimulation of their excitatory inputs from cortex or thalamus with a stereotyped response consisting of an initial EPSP with mono- and polysynaptic components which may or may not give rise to a spike, as illustrated in figure 3B. The EPSP is followed by a prolonged hyperpolarization lasting 150–300 ms which is followed by a late depolarization [Buchwald et al., 1973; Calabresi et al., 1990b; Kitai, 1981; Morris et al., 1979; Vandermaelen and Kitai, 1980; Wilson, 1992b; Wilson et al., 1983a]. Although originally suspected to be an IPSP [Buchwald et al., 1973], the long-lasting hyperpolarization has been shown to be due to disfacilitation of tonic cortical and thalamic excitatory in-

puts and corresponds to the down state in spontaneous activity [Wilson, 1992b; Wilson and Kawaguchi, 1996; Wilson et al., 1983a].

In neonates, although synaptic responses could be readily evoked from stimulation of prefrontal cortical white matter or intralaminar thalamus in all neostriatal neurons, including those recorded in the youngest animals (i.e., PD 6), they usually consisted only of a simple EPSP that sometimes gave rise to an action potential. Almost all of the neostriatal neurons (i.e., 94%, n = 164) recorded in neonates younger than PD 21 lacked the long-lasting hyperpolarization succeeding the initial EPSP as well as the late rebound excitation present in pups older than PD 25 and in adults, as shown in figure 3A. The proportion of neurons exhibiting these latter two components increased throughout postnatal development.

In individual neurons, the concordance between the long-lasting hyperpolarization following cortical and/or thalamic stimulation and the appearance of up and down states in membrane potential was striking. If a neuron exhibited disfacilitation following cortical or thalamic stimulation, it invariably showed spontaneous shifts to up and down states in membrane potential. Conversely, if a neuron did not show one of these properties it did not exhibit the other one.

Interestingly, neither the mean maximal amplitude of the EPSP nor the mean duration of the EPSP changed over development, although the onset latency became significantly shorter during the first 4 postnatal weeks. The developmental time course of EPSP characteristics is summarized in table 2.

Table 1. Waveform of spontaneous action potentials changes over postnatal development

Age	Action potential amplitude, mV	Action potential threshold, mV	Rate of rise V/s	Rate of repolarization, V/s
PD6 6–10	41.9 ± 2.1 (n = 22)*	–46.8 ± 1.7 (n = 20)	95.5 ± 28.4 (n = 5)*	49.6 ± 13.5 (n = 5)*
PD 11–15	50.6 ± 1.6 (n = 41)	–46.6 ± 1.7 (n = 26)	136.1 ± 8.7 (n = 25)*	48.5 ± 2.7 (n = 25)*
PD 16–20	58.1 ± 1.7 (n = 28)	–47.9 ± 1.5 (n = 13)	160.4 ± 15.8 (n = 16)	55.7 ± 3.1 (n = 16)*
PD 21–29	55.6 ± 1.7 (n = 70)	–46.9 ± 1.1 (n = 65)	169.9 ± 18.2 (n = 18)	57.1 ± 4.4 (n = 18)*
PD 30–40	53.0 ± 1.6 (n = 44)	–50.6 ± 1.8 (n = 23)	177.7 ± 13.2 (n = 14)	67.7 ± 3.5 (n = 14)*
Adult	56.4 ± 0.9 (n = 80)	–48.9 ± 1.2 (n = 33)	217.9 ± 15.7 (n = 13)	97.7 ± 10.7 (n = 13)

Although the mean threshold membrane potential for action potential generation does not vary as a function of postnatal age, the mean rates of rise and repolarization do not attain adult values until the 3rd and 4th weeks, respectively. Values represent mean ± SEM. Amplitudes measured from digital averages of 4 spontaneous spikes. Rates of rise and repolarization measured by digitally differentiating single spikes. Numbers in parentheses indicate number of neurons measured. * p < 0.01 vs. adult.

Fig. 3. Cortically evoked responses in medium spiny neurons in vivo change over development. **A** Prior to the end of the 3rd postnatal week, stimulation of cortex results in a simple EPSP. **B** In older pups and in adults, the same stimulus evokes an early EPSP followed by a long-lasting hyperpolarization that is succeeded by a late depolarization. **C** Cortically evoked IPSP in PD 11 medium spiny neuron in vivo. Note the decay of the IPSP over 6 min without any concomitant change in input resistance or membrane potential and the small EPSP that remains. **D** Reversal of a cortically evoked IPSP in a PD 17 pup by intracellular injection of hyperpolarizing current shows that it is a true IPSP. **E** Plot of IPSP amplitude versus membrane potential for the data in **D** reveals a reversal potential of about –60 mV, consistent with mediation by an increase in chloride conductance. **A** and **B** are single sweeps while each trace in **C** and **D** is the average of 4 sweeps.
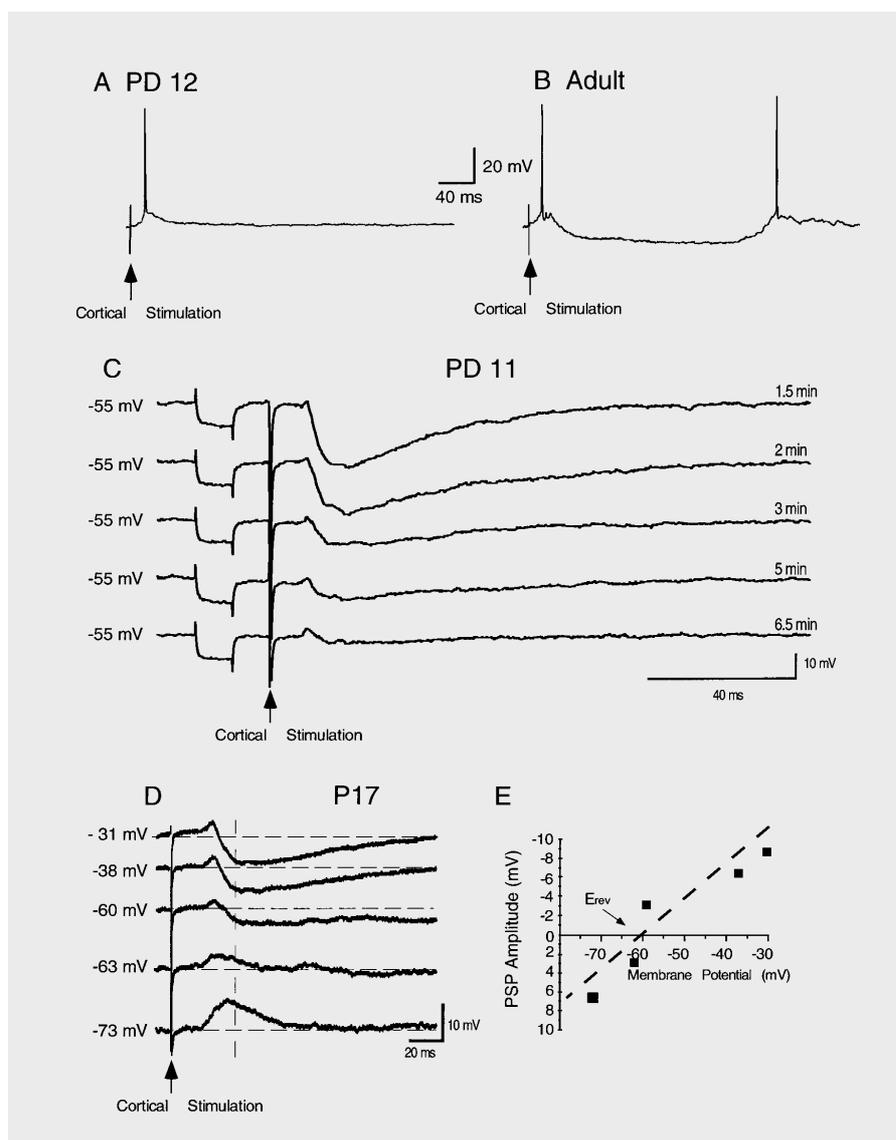
Table 2. Characteristics of cortically evoked EPSPs during postnatal development

Age	Onset ms	Rise time ms	Maximum amplitude, mV	Duration ms
PD 6–10	7.9±0.7 (n = 27)*	10.4±1.6 (n = 13)	10.4±1.4 (n = 13)	45.1±3.5 (n = 17)
PD 11–15	9.7±0.3 (n = 75)*	10.1±0.6 (n = 44)	10.2±0.8 (n = 43)	50.9±3.5 (n = 63)
PD 16–20	9.0±0.5 (n = 66)*	12.7±0.8 (n = 35)	9.9±1.1 (n = 30)	52.4±4.0 (n = 53)
PD 21–29	7.2±0.4 (n = 58)*	12.7±0.8 (n = 35)	10.3±0.9 (n = 39)	46.4±1.6 (n = 56)
PD 30–40	5.4±0.4 (n = 42)	17.9±2.5 (n = 34)*	10.6±0.9 (n = 31)	52.2±1.8 (n = 42)
Adult	5.3±0.3 (n = 69)	12.0±0.5 (n = 50)	9.5±0.8 (n = 46)	47.6±1.6 (n = 69)

Measurements are expressed as mean ± SEM. Numbers within parentheses represent numbers of cells. * $p < 0.01$ vs. adult.

One particularly unusual physiological response of neonatal medium spiny neurons was a prominent hyperpolarizing synaptic potential in response to cortical or thalamic stimulation. This was observed in 58 out of 156 neurons (37%) recorded in animals 15 days of age or younger. It was observed less frequently in the 3rd postnatal week and was never observed in animals older than PD 23. The onset latency of the hyperpolarizing potential was difficult to measure exactly because the hyperpolarization was preceded by approximately 4 ms by an EPSP in 49 of the 58 neurons. Taking the point at which the membrane potential hyperpolarized below the prestimulus baseline as the onset latency yielded a value of 12.8 ± 0.5 ms. The onset latency of the preceding EPSP was 8.8 ± 0.4 ms, which was identical with the onset latency of pure EPSPs elicited from cortex in PD 6–15 pups (table 2). One of the most unusual aspects of this response was its ephemeral nature. If it occurred at all, the hyperpolarization was present immediately upon impalement and began to decay almost immediately as shown for one example from a PD 11 pup in figure 3C. Within 5–10 min, the hyperpolarizing response was gone, leaving a small EPSP. The disappearance of the response was not due to a deterioration of the intracellular recording, as input resistance and membrane potential remained constant, and was not dependent on repeated stimulation. The response decreased in amplitude with membrane hyperpolarization and increased with depolarization as shown in figure 3D, E, indicating that it was an IPSP. The mean reversal potential was -61 ± 3.9 mV (n = 19), suggesting that it was mediated by an increase in conductance to chloride, and was thus most likely a GABA$_A$ synaptic response.

In vitro Whole Cell Recordings. Visually guided whole cell recordings were used to analyze the synaptic interaction between pairs of medium spiny neurons and pairs of fast spiking interneurons and medium spiny neurons in brain slices taken from rat pups between PD 14 and PD 37. Both cell types were targeted based on their appearance under IR-DIC and they were subsequently identified by electrophysiological criteria. The neurons were intracellularly labeled with biocytin and several of them were recovered. The morphology of the neurons always matched up with their electrophysiological identification and one neuron which was tested proved to be parvalbumin-immunoreactive, as reported previously [Kawaguchi, 1993; Kawaguchi et al., 1995].

Consistent with our in vivo findings the intrinsic properties of medium spiny neurons recorded in vitro changed dramatically, primarily during the first 3 and to a lesser extent during the 4th postnatal week. In contrast, the physiological properties of fast spiking interneurons changed very little between PD 14 and PD 29. These neurons were characterized by their ability to fire very narrow action potentials at high frequencies. The morphology of these cells did not change over this period and features characteristic for developing medium spiny neurons (e.g., varicose dendrites) were not observed. These interneurons had extremely dense axon collateral arbors (considerably denser than those of medium spiny neurons) overlapping with their dendritic field, as shown in a representative photomicrograph in figure 8.

Fifteen pairs of medium spiny neurons were recorded between PD 14 and PD 37. Spike-triggered averaging of 10–50 responses at several different postsynaptic membrane potentials was used to test for the presence of synaptic responses. No synaptic interactions were ever observed, despite the existence of a well-developed medium spiny neuron axon collateral system even in the youngest neonates [e.g., Tepper and Trent, 1993]. This finding is consistent with the study of Jaeger et al. [1994] which also failed to demonstrate synaptic interaction between medium spiny cells in the adult neostriatum. Electrotronic interactions were also tested for but not detected in any of the pairs.

Pairs of fast spiking interneurons and medium spiny neurons (youngest PD 14, oldest PD 26) were also examined. In approximately one quarter of the pairs recorded, stimulation of the fast-spiking interneuron produced IPSPs in the medium spiny neuron [Johnson et al., 1997], two examples of which are shown in figure 4. This synaptic connection was never reciprocal (i.e., IPSPs were never evoked in the interneuron by stimulation of a medium spiny neuron). Of 10 interacting cell pairs, 3 were obtained in animals between PD 22 and PD 26. The IPSP was mediated by GABA$_A$ receptors as it was reversibly blocked by the selective GABA$_A$ antagonist, bicuculline (20–50 μM; n = 3). The amplitude of the response was variable, but failures were rare (<30% in any pair). Most interestingly, the response amplitude varied significantly with age. In animals younger than PD 19 the average resonse was several millivolts in amplitude when evoked at the resting membrane potential while during the 4th week of age the resting average amplitude was in all cases less that 0.5 mV. The difference between the IPSP amplitudes in younger and older neonates was smaller if the IPSPs were compared at spike threshold (~–45 to –50 mV), where the input resistance of younger and older medium spiny neurons is less different than at rest. This observation suggests that the apparent decrease of IPSP amplitude over development reflects, at least in part, the
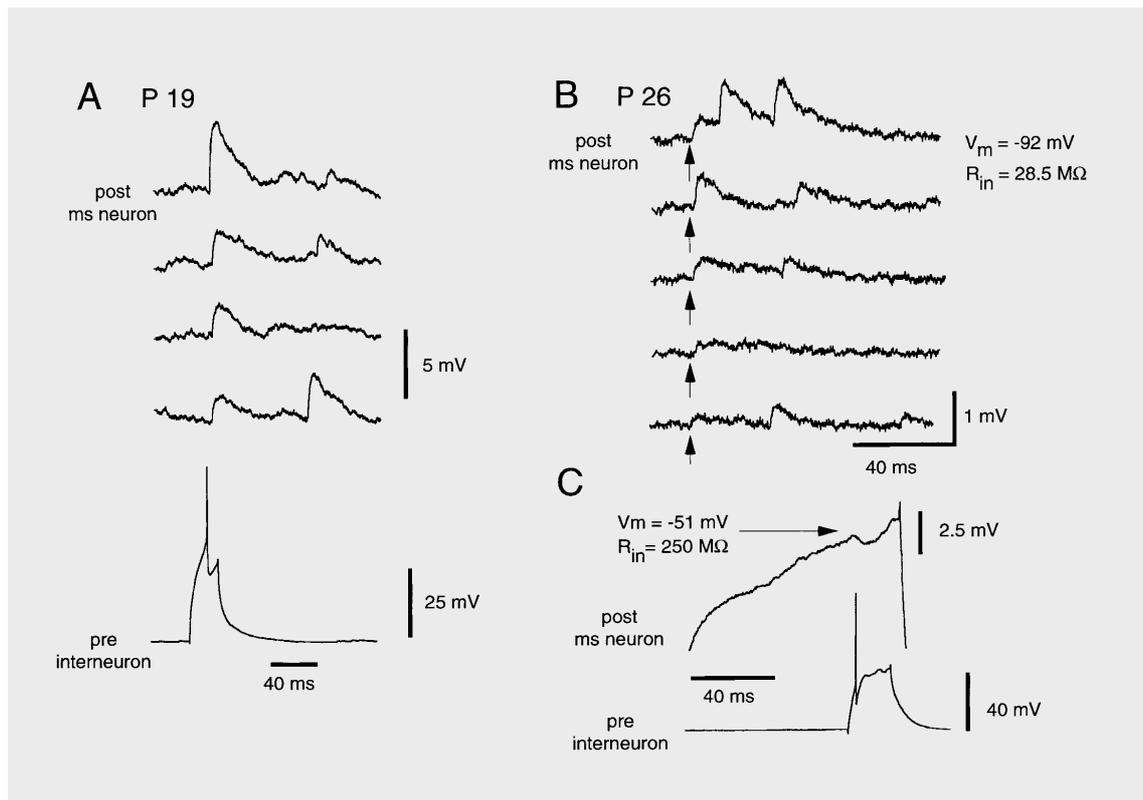
Fig. 4. Amplitude of IPSP elicited in medium spiny neuron (post ms neuron) by depolarization-induced spiking in fast spiking interneuron (pre interneuron) in vitro decreases over development. **A** Typical inverted IPSPs elicited at resting membrane potential (–77 mV) in a PD 19 medium spiny neuron recorded in whole cell mode in vitro by a single spike in the interneuron are several mV in amplitude. **B** By PD 26 the amplitude of the evoked IPSPs evoked at rest is much smaller. Note difference in calibration markers. **C** Same neuron pair as in **B**. If the older medium spiny neuron is depolarized to near spike threshold removing most of the inward rectification present at rest (compare the input resistances at the two membrane potentials), the difference in amplitude of the IPSPs at the two ages is much less. Although the amplitude of the IPSP still appears less than in the younger animal, note that the driving force on the IPSP is much reduced (e.g., the reversal potential of the IPSP is –57 mV so the driving force in the PD 19 neuron is 20 mV while in the PD 26 neuron at –51 mV it is only 6 mV).

decrease in input resistance of medium spiny cells over this period.

Light-Microscopic Observations on Neurons Intracellularly Labeled in vivo

Seventy-five neostriatal neurons were intracellularly injected with biocytin in vivo and recovered in neonates ranging from PD 6 through PD 40 and in adults. All but one were classified as medium spiny neurons based on morphological criteria including an axon that was seen to project beyond the striatum.

Medium spiny neurons in the adult rat have a characteristic appearance that has been described previously several times based on Golgi staining and intracellular labeling with HRP or biocytin [e.g., Bishop et al., 1982; Chang et al., 1982; Kawaguchi et al., 1990; Kitai, 1981; Preston et al., 1980; Walsh et al., 1989; Wilson and Groves, 1980, 1981]. Virtually identical characteristics are also displayed by medium spiny neurons in feline and primates, including man [e.g., Braak and Braak, 1982; Cepeda et al., 1994; DiFiglia et al., 1976; Fisher et al., 1986; Graveland et al., 1985; Hull et al., 1981; Izzo et al., 1987]. These include a medium-sized round or polygonal cell body from which 4–8 thick, smooth primary dendrites emerge. Within 20–30 μm from their origin the dendrites become densely spiny, with up to 4 spines/μm of length at the peak near 80 μm from the cell body [Wilson et al, 1983b]. The dendritic arborization is roughly spherical unless distorted by fiber bundles, capillaries or the boundaries of striatal neurochemical compartments,
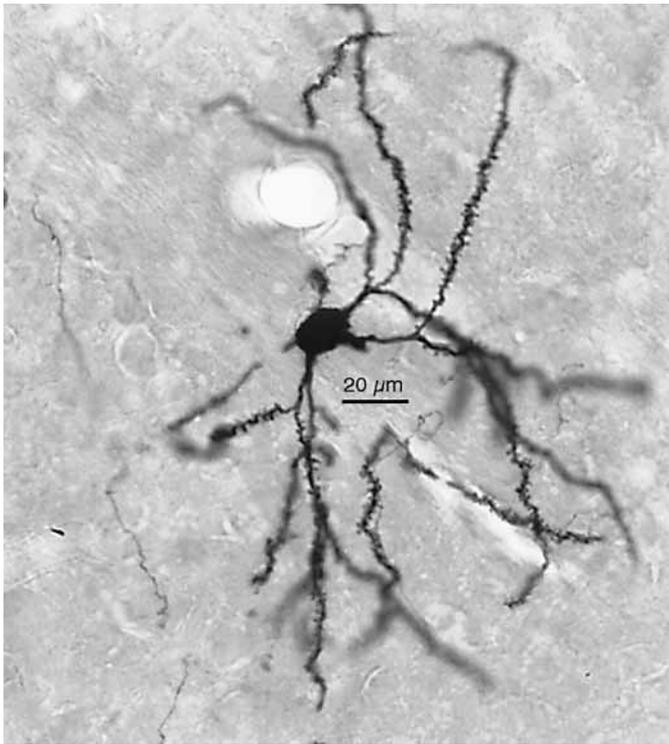
Fig. 5. Photomicrograph of a 60-µm section containing a medium spiny neuron intracellularly labeled in vivo with biocytin from an adult rat.
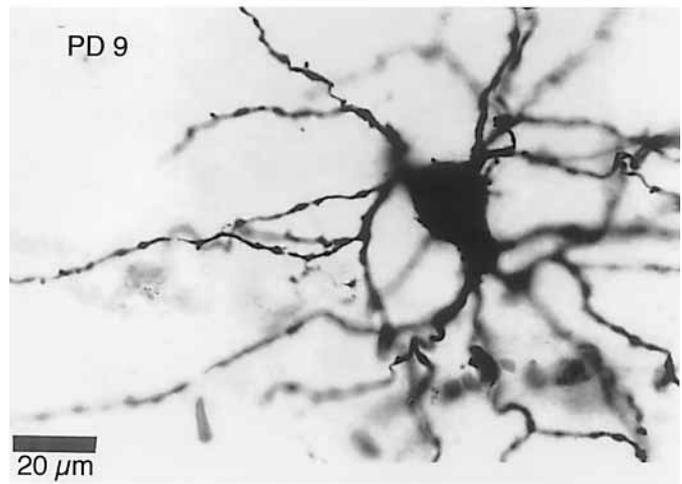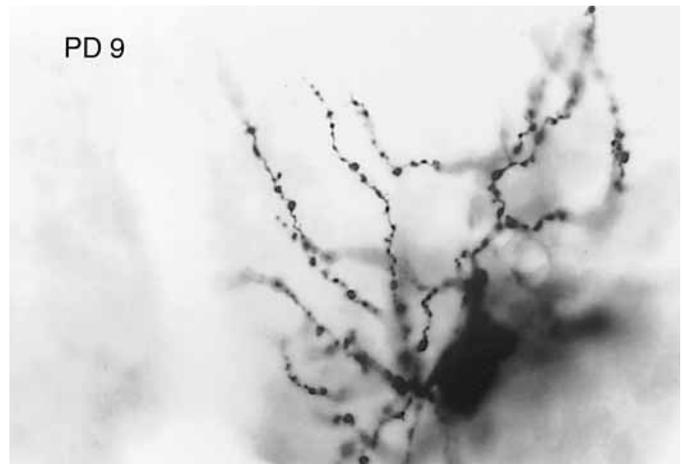
Fig. 6. Photomicrographs of 2 different medium spiny neurons intracellularly labeled with biocytin in vivo from 2 different rats at PD 9. Note the varicose dendrites and infrequent spine-like dendritic appendages.

encompassing an area of approximately 500 µm in diameter. The axon emerges from the cell body and issues a number of local collaterals resulting in a fairly dense local axon collateral plexus that in some cases is largely overlapping but more extensive than the dendritic arbor and which in others extends far beyond the dendritic field of the parent cell [Kawaguchi et al., 1990]. A photomicrograph of a medium spiny neuron from an adult rat intracellularly labeled with biocytin in vivo is shown in figure 5.

In neonatal rats medium spiny neurons appeared quite different and could only be identified reliably by the presence of an axon that could be traced out of neostriatum. During the first 2 postnatal weeks, the dendrites are relatively thin, varicose and almost completely aspiny as shown for two PD 9 neurons in figure 6. Dendritic appendages bearing an immature, globular appearance and possessing large bulbous heads that arose from thick stalks

were occasionally encountered. These membranous extensions frequently originated from or in the vicinity of dendritic varicosities. Despite this immature appearance of dendrites during the first 2 postnatal weeks, no growth cones were ever observed, consistent with previous findings in rats [Adinolfi, 1977; Lu and Brown, 1977].

During the next 2 weeks, the dendrites gradually lost their varicose appearance and the density of spines on the intermediate and distal dendrites increased. Although attempts to measure dendritic spine density quantitatively were not made, qualitative evaluation suggested that spine density increased most dramatically between PD 12 and PD 20 and that additional spines continued to appear through the 4th postnatal week. Spine densities in the PD 30–40 group appeared indistinguishable from adults [see fig. 9 in Tepper and Trent, 1993]. Although on rare occasions spines were present on the somatic and/or proximal dendritic membranes, the differential distribution
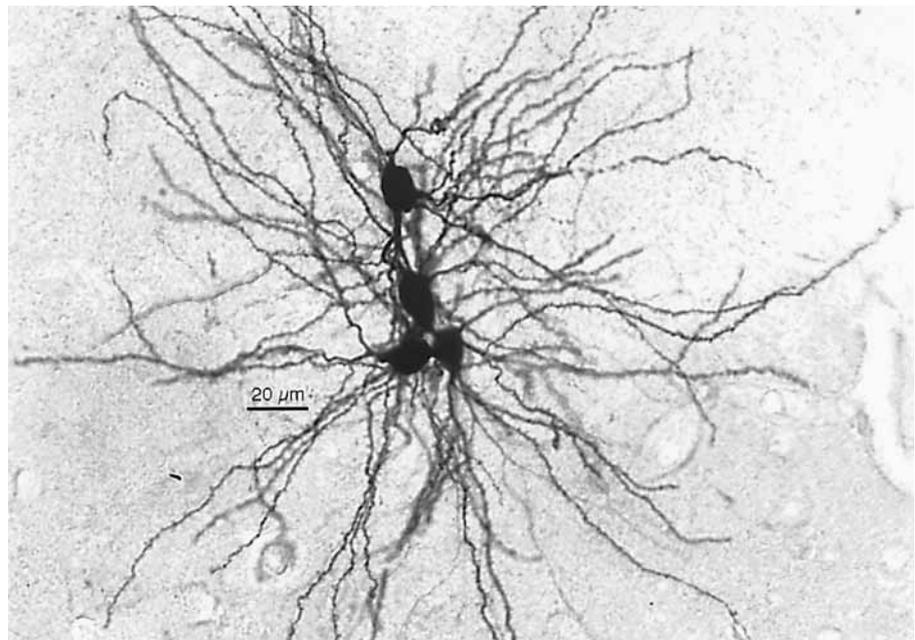
Fig. 7. Multiple neuronal labeling in a PD 19 rat following intracellular injection of biocytin into a single neuron. Note the absence of astrocytic labeling or extracellular reaction product that often accompanies poor or leaky impalements. Note also the low spine density of the dendrites.

Table 3. In contrast to the dramatic differences in spine density during the postnatal period, other morphometric parameters do not change significantly over postnatal development

Age	Mean somatic projection area µm^2	Number of primary dendrites	Number of dendritic tips	Distance to first dendritic branch µm	Mean dendritic field diameter µm	Mean axonal field diameter µm
PD 6–10	139.3 ± 14.0 (n = 17)	6.3 ± 0.7 (n = 7)	33.6 ± 3.0 (n = 5)	22.8 ± 0.9 (n = 7)	269.5 ± 17.5 (n = 6)	227.5 ± 19.4 (n = 5)
PD 11–15	159.1 ± 28.1 (n = 8)	6.7 ± 0.2 (n = 6)	28.8 ± 4.2 (n = 5)	23.8 ± 2.4 (n = 5)	272.3 ± 20.8 (n = 5)	235.7 ± 9.3 (n = 3)
PD 16–20	165.3 ± 8.8 (n = 9)	6.0 ± 0.4 (n = 7)	37.0 (n = 1)	22.8 ± 1.8 (n = 2)	308.0 (n = 1)	297.5 (n = 1)
PD 21–29	147.3 ± 11.3 (n = 14)	5.8 ± 0.3 (n = 13)	25.8 ± 1.7 (n = 11)	22.3 ± 0.8 (n = 12)	293.0 ± 7.8 (n = 11)	282.6 ± 11.8 (n = 4)
PD 30–40	142.4 ± 11.7 (n = 19)	6.3 ± 0.3 (n = 4)	34.8 ± 1.6 (n = 4)	24.1 ± 1.8 (n = 4)	318.5 ± 30.9 (n = 4)	337.8 ± 75.3 (n = 2)
Adult	147.6 ± 16.1 (n = 11)	5.7 ± 0.3 (n = 6)	32.7 ± 2.5 (n = 6)	24.2 ± 1.5 (n = 6)	290.5 ± 16.9 (n = 6)	241.5 ± 3.5 (n = 2)

All measurements were obtained from complete camera lucida reconstructions of in vivo intracellularly labeled neurons and revealed that the size of somata, and both dendritic and local axon collateral fields appear fully developed no later than PD 6 as indicated by lack of significant growth in their respective field diameters. Measurements are expressed as mean ± SEM. Numbers within parentheses represent numbers of cells measured.

in spine density along the length of the dendrite that is observed in adults was present from the initial detection of dendritic spines through adulthood.

In young neonates, multiple labeled cells often resulted from a single intracellular biocytin injection, even when the intracellular impalement appeared to be stable and secure, an example of which is shown in figure 7. This was particularly true when relatively large (>3 nA) injection currents were used. The frequency of occurrence of multi-ple labeling decreased over postnatal development and was not observed following stable intracellular impale-ments and biocytin injections in adults.

Despite the marked changes in the dendritic morphol-ogy of medium spiny neurons, in other respects these neu-rons exhibited surprisingly few changes from the earliest stained neurons (PD 6) through adulthood, as shown in table 3. There were no significant developmental changes in somatic area, the number of primary dendrites or den-
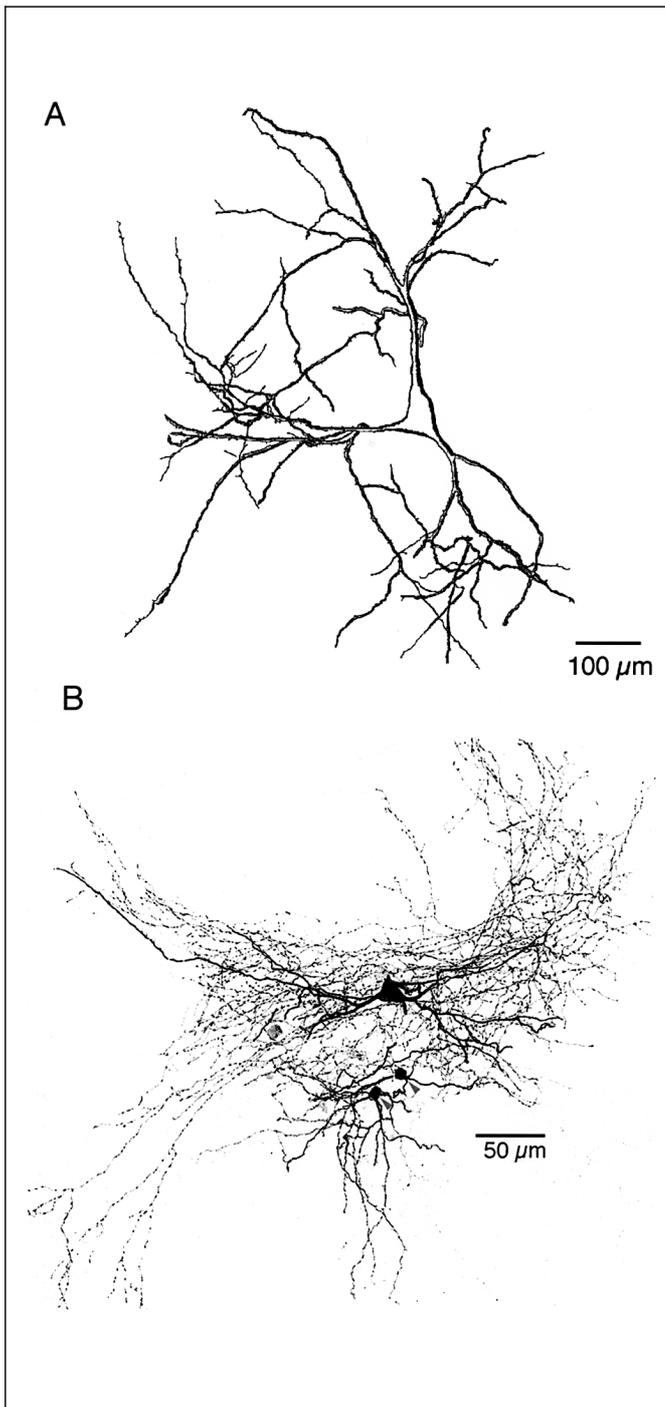
Fig. 8. Interneurons from neonatal neostriatum. **A** Partial reconstruction (i.e., from three 60-μm sections only) of the dendritic tree of a giant aspiny neuron recorded in a PD 15 pup. Note the mature appearance of the dendrites with respect to caliber and the absence of varicosities. **B** Photomicrograph of electrophysiologically identified fast-spiking interneuron and two medium spiny neurons in a 30-μm section from a PD 17 rat pup (arrowheads) labeled with biocytin during dual whole cell recording in vitro. Note the very dense local axon collateral arborization of the interneuron.

dritic tips, the distance to the first dendritic branch point, or the dendritic or axonal field diameter. Axonal growth cones were not observed at any age.

There was some variability in the observed maturity of different medium spiny neurons stained within the same animal. In many cases, this could be attributed to the location of the stained neuron within the striatum. In general, neurons appeared to develop along caudorostral and mediolateral gradients, with the most mature neurons situated medially and caudally within the striatum. There was little evidence of a ventrodorsal gradient. The state of morphological maturity was closely correlated with that of electrophysiological maturity.

Not all neuronal types within striatum mature at the same rate. Although only one interneuron was stained in vivo and recovered, a giant aspiny neuron in a PD 15 rat, the dendritic morphology of this neuron appeared much more mature than that of medium spiny neurons at this age as shown in the reconstruction in figure 8A. The morphology of this neuron resembles closely giant aspiny neurons intracellularly stained in adult rats [Wilson et al., 1990a], consistent with the earlier birthdate of cholinergic neurons [Phelps et al., 1989] than medium spiny neurons. In addition, fast spiking interneurons stained in vitro exhibited a mature morphological appearance early in the 3rd postnatal week, as shown in figure 8B. Thus, it appears that at least some of the interneurons in the striatum mature earlier than the projection neurons.

Electron Microscopic Observations

Asymmetric Synapses. The density and relative distribution of asymmetric and symmetric synapses were compared among adult, PD 21, PD 15 and PD 10 rats. An increase in the density of asymmetric synapses over postnatal development was noted (F = 8.0, df = 3, 113, p < 0.01). The density of asymmetric synapses was significantly greater in adults than at PD 15 or PD 10 (p < 0.01), but not at PD 21. The greatest increase in the density of asymmetric synapses occurred during the 3rd postnatal week, between PD 15 and PD 21 as shown in figure 11.

The increased density of asymmetric synapses in the adult neostriatum was entirely due to an increase in the density of axospinous synapses. The density of asymmetric axospinous synapses increased significantly during development (F = 33.3, df = 3, 113, p < 0.01) and was significantly greater in adults than at all other ages (p < 0.01 for all comparisons), as summarized in figure 11. In contrast, the density of axodendritic asymmetric synapses did not differ significantly among adults or neonatal rats at any age as shown in figure 11.
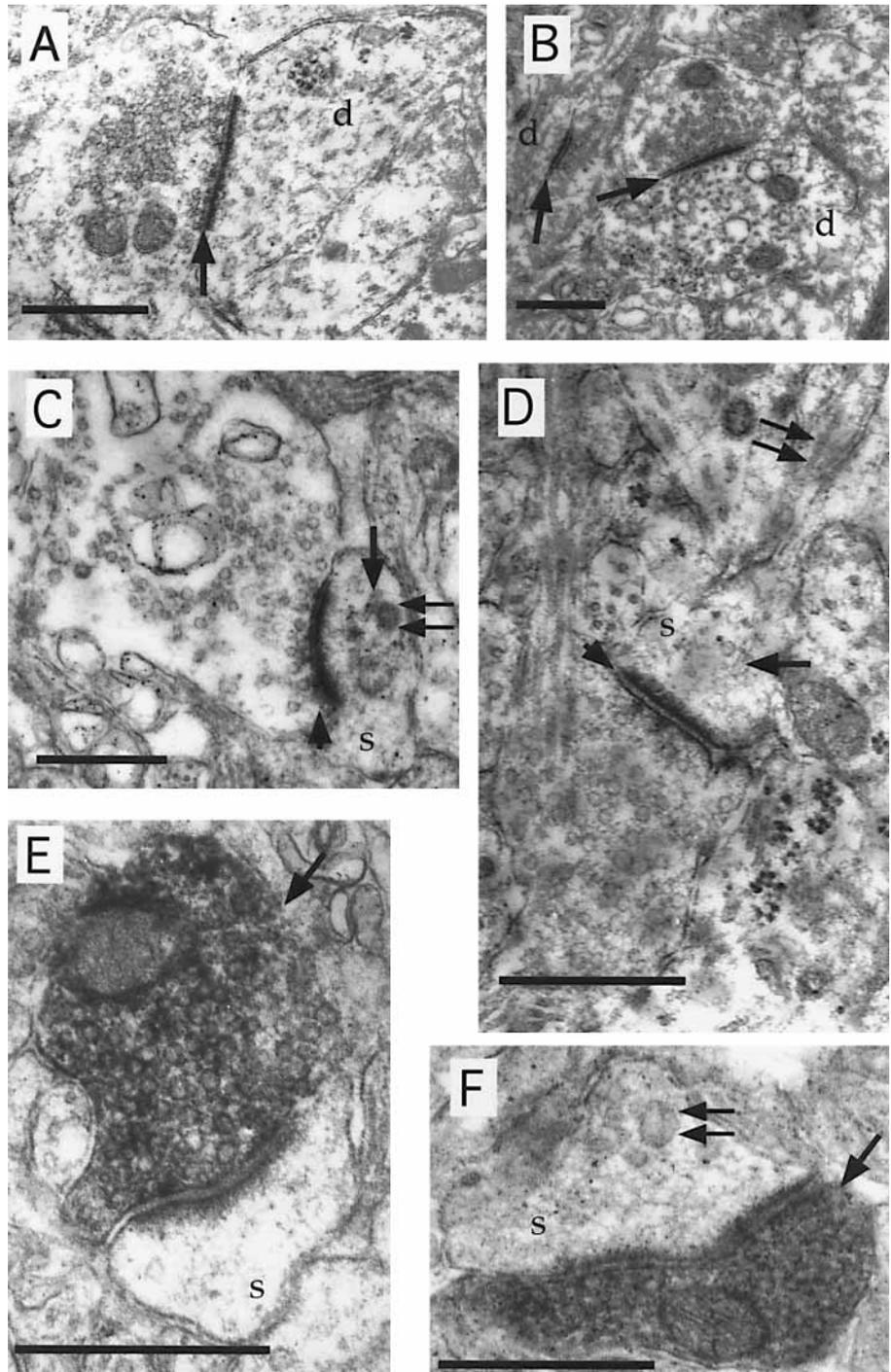
Fig. 9. Electron micrographs of asymmetric axodendritic (**A, B**) and axospinous (**C–F**) synapses in neonatal and adult rat neostriatum. **A, B** Asymmetric axodendritic synapses (arrows) at PD 10. Note that in both **A** and **B** the postsynaptic dendrites (d) are well defined and the synapses are well developed. Also note the relatively densely packed synaptic vesicles in the presynaptic profiles in comparison to axospinous profiles at PD 10 (**C**) and PD 15 (**D**). **C** Asymmetric axospinous synapse (arrowhead) onto an immature dendritic spine (s) at PD 10. Note the presence of both a microtubule fragment (arrow) and large round vacuole (double arrow) in the dendritic spine. The presence of both structures has been associated with immature dendritic spines [Westrum et al., 1980]. **D** Asymmetric axospinous synapse (arrowhead) at PD 15 onto an immature dendritic spine (s). Note the presence of a microtubule in the spine head (arrow) and spine neck (double arrow) and the relatively loose packing of synaptic vesicles in the presynaptic profiles. **E** In an adult a typical biocytin-labeled corticostriatal synaptic profile (arrow) terminates on a dendritic spine (s). Note the densely packed small round synaptic vesicles in the presynaptic bouton. **F** At PD 15 a biocytin-labeled bouton (arrow) makes an asymmetric synapse onto an immature spine head (s). The spine head is considered immature due to the presence of a large round vacuole similar to that noted in **C** (double arrow). Scale bars = 0.5 μm.

Comparing the ratio of asymmetric axospinous or axodendritic synapses to the total number of asymmetric synapses (relative synaptic organization) revealed that axodendritic synapses comprised 7% of the asymmetric synapses in the adult neostriatum while comprising 13, 41 and 67% in the PD 21, PD 15 and PD 10 neostriatum, respectively. In addition, axodendritic synapses noted throughout postnatal development appeared to be relatively more mature in terms of the length of the active zone, the density of synaptic vesicles and the area of the presynaptic bouton than axospinous synapses at the same age [Sharpe and Tepper, 1998] as shown in figure 9A and
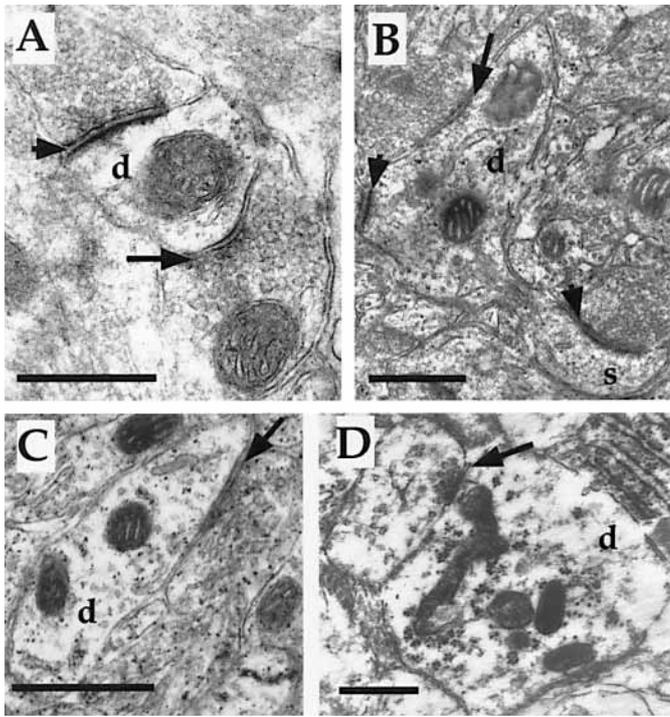
Fig. 10. Electron micrographs of symmetric synapses from adult and neonatal neostriatum. **A** Well-defined symmetric axodendritic synapse (arrow) in an adult. Note the presence of a presynaptic bouton forming an asymmetric synapse (arrowhead) onto the same dendrite (d). **B** Symmetric axodendritic synapse (arrow) at PD 21. This symmetric synapse appears similar to that noted in the adult (**A**). Note the presence of two asymmetric synapses (arrowheads), one on the same dendrite (d) as the symmetric synapse while the other is formed with the dendritic spine (s) emanating from the parent dendrite. **C** Presynaptic bouton containing pleomorphic synaptic vesicles forms symmetric synapse (arrow) on a dendrite (d) at PD 15. **D** Symmetric synapse (arrow) between a bouton containing round synaptic vesicles and a large dendrite (d) at PD 10. Scale bar = 0.5 μm.

B. The decrease in the proportion of axodendritic synapses was not the result of decrease in the density of axodendritic synapses but resulted from a significant increase in the density of axospinous synapses.

Axospinous synapses comprised 89% of the asymmetric synapses in adults and 82, 57 and 30% at PD 21, PD 15, and PD 10, respectively. The postsynaptic targets of the remaining synaptic profiles were unidentifiable. Approximately 50% of the axospinous profiles noted at PD 15 and PD 10 were with dendritic spines that were considered to be immature due to the presence of microtubules and/or large round vacuoles (considered to be immature spine apparati [Westrum et al., 1980]) as shown in fig-

ure 9C, D and F. Additionally the number of synaptic vesicles per synaptic profile was significantly greater for adults compared to PD 10 for axospinous synapses. These findings are contrasted by asymmetric axodendritic synapses which showed little change in the number of synaptic vesicles per profile over postnatal development [Sharpe and Tepper, 1998] as shown in figure 9C–F. These data suggest that asymmetric axodendritic synapses may mature earlier than axospinous synapses. Thus, it is likely that prior to PD 15 asymmetric axodendritic synapses are the primary functional excitatory input to both spiny and aspiny striatal neurons.

The postnatal development of corticostriatal boutons anterogradely labeled with biocytin was essentially identical to that of unlabeled asymmetric synapses. Biocytin-labeled corticostriatal synaptic profiles formed asymmetric membrane specializations at all ages evaluated. Corticostriatal fibers most often terminated on spine heads in adults (87%) and at PD 21 (83%), which is in good agreement with that noted for unlabeled asymmetric synapses. All other corticostriatal fibers terminated onto dendritic shafts, the necks of dendritic spines or on unidentified postsynaptic targets. As noted with unlabeled axospinous synapses, at PD 21 the labeled axospinous corticostriatal synapses appeared similar to those observed in adults. At PD 10 labeled terminals were generally located on dendritic shafts (43%) which were well defined and mature in appearance. In addition, at PD 15 and PD 10 several labeled terminals were noted on immature spine heads and necks as shown in figure 9F. The frequency of biocytin-labeled corticostriatal terminals was much lower in the younger neonates resulting in only a few labeled synapses being located in PD 10 and PD 15 animals.

Symmetric Synapses. In contrast to asymmetric synapses, the total density of symmetric synapses changed little over postnatal development [Sharpe and Tepper, 1995]. However, a slight rearrangement in the postsynaptic targets of symmetric synapses was noted. The density of symmetric synapses in adult neostriatum was not significantly different from that at PD 21, PD 15 or PD 10, as shown in figure 11. The density of axodendritic symmetric synapses changed significantly over development (F = 3.8, df = 3, 39, p < 0.05) as shown in figure 11. This statistical difference was entirely attributable to a greater density of symmetric axodendritic synapses at PD 15 than at other ages including adults. There were no significant changes in the distribution of axospinous symmetric synapses among PD 15, PD 21 and adults, although there appeared to be a trend towards increased density over development, and it should be noted that no axospinous

symmetric synapses were observed in the PD 10 group as shown in figure 11.

Axospinous symmetric synapses in adult and PD 21 rats typically terminated on spine necks. Symmetric synapses were occasionally observed terminating onto spine heads, proximal to asymmetric synapses. Symmetric synapses in the adult were evenly distributed between dendrites (35%) and spine necks (29%). At PD 21, PD 15 and PD 10 the majority of symmetric synapses were axodendritic (65, 93, and 62%, respectively). Symmetric axodendritic synapses seen as early as PD 10 appeared mature as shown in figure 10.

These data suggest that by the earliest age evaluated (PD 10), symmetric synapses are relatively mature. These findings are in sharp contrast to those noted for asymmetric synapses, particularly axospinous synapses, which do not begin to become mature until the end of the 3rd postnatal week.

Discussion

The electrophysiological, light- and electron-microscopic data all demonstrate a relatively delayed and prolonged period of postnatal development of the rat neostriatum. This protracted postnatal maturation of neostriatum, which involves both the intrinsic cellular elements as well as the extrinsic afferents, also takes place in every other mammalian species studied thus far [e.g., Cepeda et al., 1991; DiFiglia et al., 1980; Hull et al., 1981; Levine et al., 1982, 1986; Morris et al., 1979; Tanaka, 1980]. However, the time course of the postnatal development, as well as some of the specifics, varies among species.

Postnatal Development of Neostriatal Neuron Morphology

Changes in morphology of single neostriatal neurons were measured in cells intracellularly labeled with biocytin in vivo. The most significant developmental changes in rat medium spiny neurons occurred with respect to the morphology of individual dendrites. During the first 2 postnatal weeks, the neurons are essentially aspiny, and possess varicose dendrites [Trent and Tepper, 1993]. Similar findings have also been reported for medium spiny neurons during late prenatal and early postnatal development in other mammals [Adinolfi, 1977; Chronister et al., 1976; DiFiglia et al., 1980; Hull et al., 1981; Levine et al., 1986; Lu and Brown, 1977; Tanaka and Alexander, 1978; Tanaka, 1980]. Until the end of the 4th postnatal week the
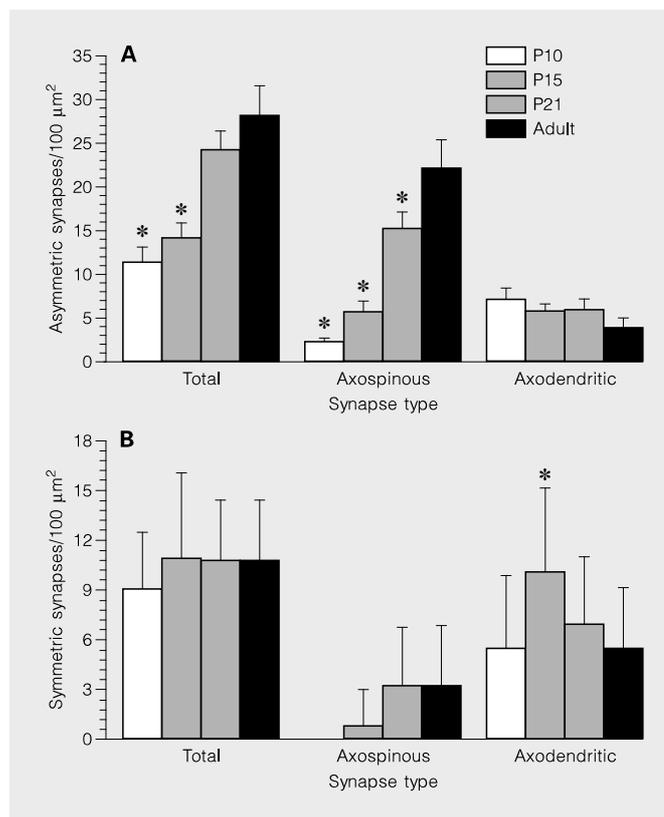

Fig. 11. A Density of asymmetric synapses from adult and neonatal rat neostriatum. Note that the total density of asymmetric synapses (axospinous plus axodendritic) and the density of axospinous synapses at PD 10 and PD 15 are significantly lower than in adults while only the density of axospinous synapses is significantly lower at PD 21. In marked contrast to axospinous synapses, the density of axodendritic synapses did not change over postnatal development. **B** Density of symmetric synapses from adult and neonatal rat neostriatum. Total density (axospinous plus axodendritic) does not change over postnatal development. The density of axodendritic synapses at PD 15 is significantly greater than in adults while the density of axospinous synapses does not change significantly. No symmetric axospinous synapses were noted at PD 10. * p < 0.01 vs. adult.

dendrites appear less spiny than in the adult, a time course that matches up well with the postnatal development of asymmetric synapses [Hattori and McGeer, 1973; Sharpe and Tepper, 1998].

One significant difference between the postnatal development of medium spiny neurons in rats and many other species is that the number of dendrites, dendritic tips and the radius of dendritic and local axonal fields of medium spiny neurons in rodents do not change appreciably, at least after PD 6–10, whereas those in felines and primates do. Feline medium spiny neurons exhibit an increase in

the radius of the dendritic and axonal arborizations over postnatal development, coupled with a modest but statistically significant decrease in the number of dendrites [Hull et al., 1981; Levine et al., 1986].

Although more than one neuron was often labeled (maximum 4 labeled cells, see fig. 7) in early neonates following what appeared to be stable intracellular impalements, multiple labeling was not observed past 21 days of age. A similar decrease in the incidence of dye coupling over development has been reported previously when using lucifer yellow as the intracellular dye in vitro studies [Cepeda et al., 1991; Walsh et al., 1989]. The decrease in dye coupling has been interpreted to indicate a decrease in gap junction permeability and electrotonic coupling as maturation occurs. While this remains a distinct possibility, especially since the degree of dye coupling in neostriatum has been reported to be altered by manipulations of the dopaminergic system [e.g., Cepeda et al., 1989; Onn and Grace, 1994], it may also reflect the increased stability of the intracellular penetration as the striatum becomes more heavily myelinated and neurons and processes acquire a more extensive glial sheath. In our in vitro recordings, we did not observe any multiple biocytin labeling, even in slices from rats in the 2nd and 3rd postnatal week, nor did we observe any evidence of electrotonic coupling between pairs of medium spiny neurons, despite the fact that electrotonic coupling was readily observed between a pair of fast-spiking interneurons [Johnson et al., 1997]. Furthermore, although electron-microscopic evidence of gap junctions between medium spiny neurons is scarce, gap junctions have been readily detected between pairs of parvalbumin-containing (i.e., fast-spiking) striatal interneurons [Kita, 1993]. In addition, it should be noted that we never observed multiple labeling of fast-spiking interneurons following biocytin injection into one interneuron.

There was evidence for a gradient of morphological maturation that proceeded from caudal to rostral and medial to lateral, which was paralleled by indices of electrophysiological maturation. This most likely results from a similar gradient with respect to neuronal birthdate [Bayer, 1984; Phelps et al., 1989]. It is interesting to note both the time course of postnatal development of neostriatal neurons as well as the caudorostral spatial gradient are paralleled in neostriatum by a replacement or change in expression of nerve cell adhesion molecule from the 'immature' highly polysialylated form to the adult version which carries fewer sialic acid residues [Szele et al., 1994]. The polysialylated form is largely gone by PD 25. By this time medium spiny neurons appear essentially adult-like in morphology, the bulk of the afferents have

arrived and made synaptic contact, and the neurons begin to show up and down states and disfacilitation following cortical or thalamic stimulation (see below). Thus, the disappearance of the polysialylated form of NCAM may be a useful marker for the end of the most vigorous period of active synaptic growth and reconfiguration during development [Szele et al., 1994].

Postnatal Development of Neostriatal Synapses

In a classic study, Hattori and McGeer [1973] examined the postnatal development of synapses in rat striatum. They found the greatest increase in the density of synapses occurred between PD 13 and 17. Whereas the density of symmetric synapses became maximal by PD 17, the density of asymmetric synapses continued to increase beyond PD 21 (the oldest neonatal age examined) through adulthood. Our electron-microscopic results [Sharpe and Tepper, 1995, 1998] were consistent with these findings, showing in addition that the large increase in the density of asymmetric synapses was accounted for principally by new axospinous synapses. In contrast, the density of asymmetric synapses which terminated on dendritic shafts did not change over development. Studies of corticostriatal synapses labeled with biocytin gave the same results. These data suggest the possibility that the asymmetric axodendritic synapses on medium spiny neurons that are present in adults derive from cortical (and perhaps also thalamic) afferents that were the earliest to arrive and make contact during development. It is interesting to note that the corticostriatal and thalamostriatal innervation of neostriatal grafts also show an increased proportion of asymmetric synapses made onto dendritic shafts [Clarke and Dunnett, 1990; Wictorin and Bjorklund, 1989; Wictorin et al., 1989; Xu et al., 1989].

It could not be determined whether the asymmetric axodendritic synapses were made onto medium spiny neurons or aspiny interneurons present in neostriatum and it is likely that at least some of them were made onto fast-spiking interneurons. The influence of these early inputs onto fast-spiking interneurons might be significantly greater in the young neonate with respect to the generation of intrastriatal IPSPs since the corticostriatal input is not yet fully developed and the fast-spiking interneurons may be more sensitive to excitatory inputs than the medium spiny neurons [Kawaguchi, 1993; Kita, 1993].

The change in distribution of termination sites of asymmetric synapses may help explain why the mean maximal amplitude of the cortically elicited EPSP does not change over postnatal development despite a nearly 250% increase in the density of asymmetric synapses

from PD 10 to adulthood. Since most of the early excitatory synapses are made onto dendritic shafts rather than spine heads, each input will carry a greater synaptic weight since the flow of synaptic current will not be attenuated by a high resistance spine neck [Wilson, 1984]. As the later excitatory afferents arrive, they form synapses with spine heads so even though the numbers of synapses increases, these synapses are electrotonically more distant from the somatic recording site. This, coupled with the decreased input resistance as inward rectification develops and the general electrotonic lengthening of the neuron as a result of the genesis of dendritic spines [Wilson, 1984], may serve to keep the maximal size of the EPSP constant over development.

In contrast to asymmetric synapses, the density of symmetric synapses, which represent synapses made by the axon collaterals of the medium spiny neurons as well as those made by intrinsic interneurons, did not change appreciably over postnatal development. The relatively early maturation of inhibitory synapses is also likely a factor in the dominant expression of IPSPs following cortical stimulation in neonates.

Postnatal Development of Electrophysiological Properties

In terms of the maturation of the electrophysiology of the medium spiny neuron one may distinguish between properties that depend primarily on the intrinsic conductances of individual neurons and the cellular morphology versus those that also depend on afferent input. Properties of the former category comprise the presence of inward rectification, input resistance, action potential duration, amplitude and rise time and resting membrane potential. Those in the latter category include the rate and pattern of spontaneous activity and the synaptic response to cortical or thalamic inputs. In general the intrinsic neuronal properties are well-developed by the end of the 3rd postnatal week, whereas those that depend on afferent input lag behind by 1–2 weeks.

Membrane Properties. The absence of inward rectification early in the neonatal period has been previously reported in in vitro medium spiny neurons [Misgeld et al., 1986] and in other neurons that typically show inward rectification as adults [e.g., Krigstein et al., 1987; McCormick and Prince, 1987; Segal, 1990]. The absence of the inward rectification and consequent higher input resistance in neonatal rats has also been reported for feline medium spiny neurons [Cepeda et al., 1991] and the maturation of these properties has a similar time course in both species, becoming essentially adult-like by the end of

the 3rd postnatal week. The absence of inward rectification and higher input resistance in neonates has a profound effect on both spontaneous activity and synaptic responses as discussed below.

The outward rectification that dominates the IV relation of some of the neonatal medium spiny neurons most likely does not reflect the presence of a conductance that is present in the neonates but not in mature medium spiny neurons. Adult medium spiny neurons also exhibit a prominent outward rectification that is not usually seen unless sodium and calcium conductances are blocked to allow the cell to be depolarized sufficiently [Nisenbaum and Wilson, 1995; Nisenbaum et al., 1994]. Several outwardly rectifying currents have been identified in medium spiny neurons, and at least two of them have been shown to be present very early in the postnatal period [e.g., Surmeier et al., 1991]. Thus, the prominent outward rectification seen during the first 2 postnatal weeks most likely represents the delayed expression of the inward rectifier rather than the transient expression of a novel outward rectifier.

The resting membrane potential became more hyperpolarized over postnatal development, and spontaneous action potentials became larger and decreased in duration through the 3rd postnatal week. A similar developmental time course has been observed for action potentials recorded in other brain regions of neonatal rats including hippocampus, neocortex, substantia nigra, and locus ceruleus [e.g., Fukuda and Prince, 1992; Lorenzon and Foehring, 1993; McCormick and Prince, 1987; Nakamura et al., 1987; Tepper et al., 1990; Williams and Marshall, 1987]. The increase in resting membrane potential and decrease in spike duration has also been reported over postnatal development in feline neostriatum [Levine et al., 1982], and may be due in part to the relatively late development of an electrogenic sodium pump [Fukuda and Prince, 1992].

Spontaneous Activity. There is little or no spontaneous activity prior to PD 15. This has been previously reported for rat neostriatal neurons [Napier et al., 1985; Tepper and Trent, 1993] and is also characteristic of the neonatal feline striatum [Levine et al., 1982; Lidsky et al., 1976]. Discrete up and down states, as described in adult medium spiny neurons in vivo [Stern et al., 1997; Wilson and Kawaguchi, 1996], are absent in young neonates. Their appearance during development shares an identical time course with that of the disfacilitation following cortical or thalamic stimulation [Tepper and Trent, 1993] which is also absent in neonatal feline medium spiny neurons [Morris et al., 1979]. This correspondence is consistent

with the proposed identity of the neuronal mechanisms underlying both the long-lasting hyperpolarization and the down state, namely an interaction of the strong inward rectification of the medium spiny neuron and disfacilitation of tonic excitatory cortical input [Wilson, 1992b; Wilson and Kawaguchi, 1996; Wilson et al., 1983a]. The paucity of spontaneous activity, the absence of the disfacilitation and up and down states in the neonates are likely due in large part to a reduced tonic excitatory tone from cortex and thalamus suggests that even though some asymmetric synapses are present in neostriatum very early in the postnatal period, and even though these connections can be functional (see below), corticostriatal and thalamostriatal neurons must have a very low level of spontaneous activity early in the neonatal period.

Synaptic Potentials. EPSPs could be elicited by cortical or thalamic stimulation even in the earliest neonates recorded (PD 6). The characteristics of the EPSP changed relatively little over development in contrast to the succeeding phases of the evoked responses, except for onset latency, which became significantly shorter. This may be accounted for by a developmental increase in the conduction velocity of individual corticostriatal fibers, as has been documented to occur in kittens [Oka et al., 1985]. However, there are at least two different types of corticostriatal input; a rapidly conducting pathway from the collaterals of ipsilaterally projecting corticospinal neurons and a more slowly conducting one that projects bilaterally to the neostriatum [Wilson, 1995]. Thus, it is possible that the decrease in latency comes about because the earliest inputs come from the more slowly conducting corticostriatal pathway while the faster collateral pathway does not significantly innervate the striatum until later.

Cortical or thalamic stimulation evokes a complex response in adult medium spiny cells which includes a mono- and polysynaptic EPSP, a GABA$_A$ IPSP, disfacilitation and a rebound EPSP [e.g., Buchwald et al., 1973; Calabresi et al., 1990b; Kitai, 1981; Vandermaelen and Kitai, 1980; Wilson et al., 1983a]. Prior to PD 16–20, most neonatal medium spiny neurons showed only a simple EPSP in response to cortical or thalamic stimulation. The absence of the long-lasting hyperpolarization (disfacilitation) and subsequent late EPSP has also been reported for neonatal medium spiny neurons in cats [Morris et al., 1979], and is almost certainly due to a lack of tonic excitatory input from cortex in the young animals (see above).

In adults, the IPSP component of the response to cortical or thalamic stimulation is usually masked by the much larger mono- and polysynaptic EPSP components and the long-lasting hyperpolarization in in vivo recordings. Sur-prisingly, cortical stimulation often elicited a very prominent polysynaptic IPSP in medium spiny neurons in young neonates. In most cases this IPSP was, like in the adult, a mixed EPSP-IPSP complex, however, the IPSP dominated the response. This is consistent with in vitro data [Misgeld et al., 1986] showing that the development of inhibitory synaptic responses precedes the development of excitation in the rat neostriatum.

The cellular origin of the cortically or thalamically evoked IPSP could not be identified in the in vivo studies; however, it was almost certainly intrastriatal. There are several reasons to assume that the IPSP is mediated by local GABAergic interneurons rather than by the recurrent axon collaterals of the medium spiny cells themselves. First, the IPSP can be evoked with low stimulation intensity at which few if any spiny cells respond by firing action potentials. Second, it has been shown that medium spiny neurons do not inhibit each other [Jaeger et al., 1994, and present results]. Finally, at least one class of GABAergic interneuron, the parvalbumin-containing fast-spiking neuron, appears to have mature intrinsic electrophysiological properties and functional excitatory responses from the neocortex at least by the end of the 2nd postnatal week [Kawaguchi, 1993; Koós and Tepper, unpubl. observations], and these neurons evoke very large amplitude IPSPs in medium spiny neurons in neonates.

The predominance of inhibition over excitation in the neonatal neostriatum is likely to be a consequence primarily of the delayed development of the cortical and thalamic inputs and does not necessarily reflect a change in inhibitory input. This argument is consistent with our finding that the density of asymmetric but not symmetric synapses increases after PD 15 in the neostriatum. While it is possible that the functional strength of the inhibitory input to medium spiny neurons changes during development, the apparent decrease in inhibition may be only a reflection of a decrease in postsynaptic input resistance and perhaps an increase in the electrotonic length of the neuron consequent to spine development. The observation that the interneuron-evoked IPSP does not appear to be very different in younger and older medium spiny neurons when postsynaptic input resistance is held constant by altering the membrane potential supports this interpretation. As mentioned earlier, it is possible that parvalbumin interneurons establish functionally mature excitatory synaptic inputs early in development and may therefore form relatively mature feed-forward inhibitory circuitry in the neostriatum prior to the maturation of excitatory corticostriatal and thalamostriatal afferents to medium spiny neurons.

A remarkable feature of the IPSP was its transient nature. Interestingly, the same phenomenon has been observed in the case of cortically evoked IPSPs in neostriatal grafts recorded in vivo [Wilson et al., 1990b; Xu et al., 1991]. The reasons for the decay of the IPSP are unknown. However, in in vitro studies of a similar IPSP in neonates, there is no mention of this phenomenon [Misgeld et al., 1986; Walsh et al., 1988], and in our paired recordings we found no evidence of similar time-dependent decay of the interneuron-evoked IPSP in medium spiny neuron cells at any age investigated. It is possible that in vivo impalement of the medium spiny neuron results in the initiation of a process or processes that results in the failure of the coupling of ligand binding and channel opening in these cells. This process could be initiated by an elevation of intracellular calcium concentration or other damage-related biochemical changes in the neuron. It is possible that in vitro intracellular or whole cell recording eliminates the initiating factor(s) which occurs during intracellular recording in vivo.

mature are the intrinsic membrane properties. However, even these are very different within the first 3 postnatal weeks than they are in the mature animal, indicating that caution must be exercised before extrapolating electrophysiological findings obtained in neonatal animals less than 3 weeks old to those in the adult. Although the somatic size and extent of the dendritic and local axon collateral arborization of rat medium spiny neurons does not change significantly during that postnatal period, individual dendrites of medium spiny neurons are initially varicose and aspiny. Dendritic spines develop concomitantly with the arrival of the majority of corticostriatal inputs that form asymmetric excitatory axospinous synapses, which occurs during the 3rd and 4th postnatal weeks, and it is not until then that synaptic responses and spontaneous activity begin to resemble those seen in the adult. Thus, in order to be applicable to the adult striatum, studies of synaptic responses and/or network properties should be carried out in rats that are at least 4 or 5 weeks of age.

Conclusions

A number of significant changes in the electrophysiological and morphological properties of the rat neostriatum take place during the 1st postnatal month. The first to

Acknowledgments

References

Adinolfi AM (1977): The postnatal development of the caudate nucleus: A Golgi and electron microscopic study of kittens. Brain Res 133:251–266.

Bayer SA (1984): Neurogenesis in the rat neostriatum. In J Dev Neurosci 2:163–173.

Bishop GA, Chang HT, Kitai ST (1982): Morphological and physiological properties of neostriatal neurons: An intracellular horseradish peroxidase study in the rat. Neuroscience 7:179–191.

Braak H, Braak E (1982): Neuronal types in the striatum of man. Cell Tissue Res 227:319–342.

Buchwald NA, Price DD, Vernon L, Hull CD (1973): Caudate intracellular responses to thalamic and cortical inputs. Exp Neurol 38:311–323.

Calabresi P, Mercuri NB, Bernardi G (1990a): Synaptic and intrinsic control of membrane excitability of neostriatal neurons. II. An in vitro analysis. J Neurophysiol 63:663–675.

Calabresi P, Mercuri NB, Stefani A, Bernardi G (1990b): Synaptic and intrinsic control of membrane excitability of neostriatal neurons. I. An in vivo analysis. J Neurophysiol 63:651–662.

Cepeda C, Walsh JP, Buchwald NA, Levine MS (1991): Neurophysiological maturation of cat caudate neurons: Evidence from in vitro studies. Synapse 7:278–290.

Cepeda C, Walsh JP, Hull CD, Howard SG, Buchsbaum MS, Levine MS (1989): Dye-coupling in the neostriatum of the rat. I. Modulation by dopamine-depleting lesions. Synapse 4:229–237.

Cepeda C, Walsh JP, Peacock W, Buchwald NA, Levine MS (1994): Neurophysiological, pharmacological and morphological properties of human caudateneurons recorded in vitro. Neuroscience 59:89–103.

Chang HT, Wilson C, Kitai ST (1982): A Golgi study of rat neostriatal neurons: Light microscopic analysis. J Comp Neurol 208:107–126.

Chronister RB, Farnell KE, Marco LA, White LE (1976): The rodent neostriatum: A Golgi analysis. Brain Res 108:37–46.

Clarke DJ, Dunnett SB (1990): Ultrastructural organization within intrastriatal striatal grafts; in Dunnett SB, Richards SJ (eds): Progress in Brain Research. Amsterdam, Elsevier, vol 82, pp 407–415.

DiFiglia M, Pasik P, Pasik T (1976): A Golgi study of neuronal types in the neostriatum of monkeys. Brain Res 114:245–256.

DiFiglia M, Pasik P, Pasik T (1980): Early postnatal development of the monkey neostriatum: A Golgi and ultrastructural study. J Comp Neurol 190:303–331.

DiFiglia M, Schiff L, Deckel AW (1988): Neuronal organization of fetal striatal grafts in kainate- and sham-lesioned rat caudate nucleus: Light- and electron-microscopic observations. J Neurosci 8:1112–1130.

Fishell G, Van der Kooy D (1987): Pattern formation in the striatum: Developmental changes in the distribution of striatonigral neurons. J Neurosci 7:1969–1978.

Fisher RS, Buchwald NA, Hull CD, Levine MS (1986): The GABAergic striatonigral neurons of the cat: Demonstration by double peroxidase labeling. Brain Res 398:148–156.

Fukuda A, Prince DA (1992): Postnatal development of electrogenic sodium pump activity in rat hippocampal pyramidal neurons. Dev Brain Res 65:101–114.

Graveland GA, Williams RS, DiFiglia M (1985): A Golgi study of the human neostriatum: Neurons and afferent fibers. J Comp Neurol 234:317–333.

Hattori T, McGeer PL (1973): Synaptogenesis in the corpus striatum of infant rat. Exp Neurol 38:70–79.

Horikawa K, Armstrong WE (1988): A versatile means of intracellular labeling: Injection of biocytin and its detection with avidin conjugates. J Neurosci Methods 25:1–11.

Hull CD, McAllister JP, Levine MS, Adinolfi AM (1981): Quantitative development studies of feline neostriatal spiny neurons. Dev Brain Res 1:309–332.

Izzo PN, Graybiel AM, Bolam JP (1987): Characterization of substance P- and [met]enkephalin-immunoreactive neurons in the caudate nucleus of cat and ferret by a single section Golgi procedure. Neuroscience 20:577–587.

Jaeger D, Kita H, Wilson CJ (1994): Surround inhibition among projection neurons is weak or nonexistent in the rat neostriatum. J Neurophysiol 72:1–4.

Johnson LR, Koós T, Záborszky L, Moore K, Tepper JM (1997): GABA$_A$ receptor-mediated inhibition of medium spiny neurons by fast spiking interneurons in rat neostriatum. Soc Neurosci Abstr 23:1279.

Kawaguchi Y (1993): Physiological, morphological, and histochemical characterization of three classes of interneurons in rat neostriatum. J Neurosci 13:4908–4923.

Kawaguchi Y, Wilson CJ, Augood SJ, Emson PC (1995): Striatal interneurones: Chemical, physiological and morphological characterization. Trends Neurosci 18:527–535.

Kawaguchi Y, Wilson CJ, Emson PC (1990): Projection subtypes of rat neostriatal matrix cells revealed by intracellular injection of biocytin. J Neurosci 10:3421–3438.

Kemp JM, Powell TPS (1971a): The structure of the caudate nucleus of the cat: Light and electron microscopy. Philos Trans R Soc Lond B 262:383–401.

Kemp JM, Powell TPS (1971b): The synaptic organization of the caudate nucleus. Philos Trans R Soc Lond B 262:403–412.

Kemp JM, Powell TPS (1971c): The site of termination of afferent fibers in the caudate nucleus. Philos Trans R Soc Lond B 262:413–427.

Kita H (1993): GABAergic circuits of the striatum; in Arbuthnott GW, Emson PC (eds): Chemical Signalling in the Basal Ganglia. Prog Brain Res Amsterdam, Elsevier, vol 99, pp 51–72.

Kita T, Kita H, Kitai ST (1984): Passive electrical membrane properties of rat neostriatal neurons in an in vitro slice preparation. Brain Res 300:129–139.

Kitai ST (1981): Anatomy and physiology of the neostriatum; in Di Chiara G, Gessa GL (eds): GABA and the Basal Ganglia. Adv Biochem Psychopharmacol. New York, Raven Press, vol 30, pp 1–21.

Kriegstein AR, Suppes T, Prince DA (1987): Cellular and synaptic physiology and epileptogenesis of developing rat neocortical neurons in vitro. Brain Res 431:161–171.

Levine MS, Fisher RS, Hull CD, Buchwald NA (1982): Development of spontaneous neuronal activity in the caudate nucleus, globus pallidus-entopeduncular nucleus, and substantia nigra of the cat. Dev Brain Res 3:429–441.

Levine MS, Fisher RS, Hull CD, Buchwald NA (1986): Postnatal development of identified medium-sized caudate spiny neurons in the cat. Dev Brain Res 24:47–62.

Lidsky TI, Buchwald NA, Hull CD, Levine MS (1976): A neurophysiological analysis of the development of cortico-caudate connections in the cat. Exp Neurol 50:283.

Lorenzon NM, Foehring RC (1993): The ontogeny of repetitive firing and its modulation by norepinephrine in rat neocortical neurons. Dev Brain Res 73:213–223.

Lu EJ, Brown WJ (1977): An electron microscopic study of the developing caudate nucleus in euthyroid and hypothyroid states. Anat Embryol 150:335–364.

McCormick DA, Prince DA (1987): Post-natal development of electrophysiological properties of rat cerebral cortical pyramidal neurones. J Physiol 393:743–762.

Misgeld U, Dodt HU, Frotscher M (1986): Late development of intrinsic excitation in the rat neostriatum: An in vitro study. Dev Brain Res 27:59–67.

Morris R, Levine MS, Cherubini E, Buchwald NA, Hull CD (1979): Intracellular analysis of the development of responses of caudate neurons to stimulation of cortex, thalamus and substantia nigra in the kitten. Brain Res 173:471–487.

Nakamura S, Kimura F, Sakaguchi T (1987): Postnatal development of electrical activity in the locus ceruleus. J Neurophysiol 58:510–524.

Napier TC, Coyle S, Breese GR (1985): Ontogeny of striatal unit activity and effects of single or repeated haloperidol administration in rats. Brain Res 333:35–44.

Nisenbaum ES, Wilson CJ (1995): Potassium currents responsible for inward and outward rectification in rat neostriatal spiny projection neurons. J Neurosci 15:4449–4463.

Nisenbaum ES, Xu ZC, Wilson CJ (1994): Contribution of a slowly inactivating potassium current to the transition to firing of neostriatal spiny projection neurons. J Neurophysiol 71:1174–1189.

Oka H, Samejima A, Yamamoto T (1985): Postnatal development of pyramidal tract neurones in kittens. J Physiol (Lond) 363:481–499.

Onn S-P, Grace AA (1994): Dye coupling between rat striatal neurons recorded in vivo: Compartmental organization and modulation by dopamine. J Neurophysiol 71:1917–1934.

Phelps PE, Brady DR, Vaughn JE (1989): The generation and differentiation of cholinergic neurons in rat caudate-putamen. Dev Brain Res 46:47–60.

Preston RJ, Bishop GA, Kitai ST (1980): Medium spiny neurons from rat striatum: An intracellular horseradish peroxidase study. Brain Res 183:253–263.

Segal M (1990): Developmental changes in serotonin actions in rat hippocampus. Dev Brain Res 52:247–252.

Sharpe N, Tepper JM (1995): Development of inhibitory synapses in rat neostriatum. Soc Neurosci Abstr 21:1424.

Sharpe NA, Tepper JM (1998): Postnatal development of excitatory input to rat neostriatum: An electron microscopic study. Neuroscience 84:1163–1175.

Stern EA, Kincaid AE, Wilson CJ (1997): Spontaneous subthreshold membrane potential fluctuations and action potential variability of rat corticostriatal and striatal neurons in vivo. J Neurophysiol 77:1697–1715.

Surmeier DJ, Stefani A, Foehring RC, Kitai ST (1991): Developmental regulation of a slowly-inactivating potassium conductance in rat neostriatal neurons. Neurosci Lett 122:41–46.

Szele FG, Dowling JJ, Gonzales C, Theveniau M, Rougon G, Chesselet M-F (1994): Pattern of expression of highly polysialylated neural cell adhesion molecule in the developing and adult rat striatum. Neuroscience 60:133–144.

Tanaka D (1980): Development of spiny and aspiny neurons in the caudate nucleus of the dog during the first postnatal month. J Comp Neurol 192:247–263.

Tanaka D, Alexander B (1978): Golgi and electron microscopic evidence for growth cones in the caudate nucleus of the neonatal dog. Exp Neurol 60:614–623.

Tepper JM, Sawyer SF, Groves PM (1987): Electrophysiologically identified nigral dopaminergic neurons intracellularly labeld with HRP: Light microscopic analysis. J Neurosci 7:2794–2806.

Tepper JM, Trent F (1993): In vivo studies of the postnatal development of rat neostriatal neurons; in Arbuthnott GW, Emson PC (eds): Chemical Signalling in the Basal Ganglia. Prog Brain Res. Amsterdam, Elsevier, vol 99, pp 35–50.

Tepper JM, Trent F, Nakamura S (1990): Postnatal development of the electrical activity of rat nigrostriatal dopaminergic neurons. Dev Brain Res 54:21–33.

Trent F, Tepper JM (1991): Postnatal development of synaptic responses, membrane properties and morphology of rat neostriatal neurons in vivo. Soc Neurosci Abstr 17:938.

Trent F, Tepper JM (1993): Morphological development of rat neostriatal medium spiny neurons intracellularly labeled with biocytin. Soc Neurosci Abstr 19:1434.

Van der Kooy D, Fishell G (1987): Neuronal birthdate underlies the development of striatal compartments. Brain Res 401:155–161.

Vandermaelen CP, Kitai ST (1980): Intracellular analysis of synaptic potentials in rat neostriatum following stimulation of the cerebral cortex, thalamus, and substantia nigra. Brain Res Bull 5:725–733.

Walsh JP, Cepeda C, Hull CD, Fisher RS, Levine MS, Buchwald NA (1989): Dye-coupling in the neostriatum of the rat. II. Decreased coupling between neurons during development. Synapse 4:238–247.

Walsh JP, Zhou FC, Hull CD, Fisher RS, Levine MS, Buchwald NA (1988): Physiological and morphological characterization of striatal neurons transplanted into the striatum of adult rats. Synapse 2:37–44.

Westrum LE, Hugh Jones D, Gray EG, Barron J (1980): Microtubules, dendritic spines and spine apparatuses. Cell Tissue Res 208:171–181.

Wictorin K, Bjorklund A (1989): Connectivity of striatal grafts implanted into the ibotenic acid-lesioned striatum. II. Cortical afferents. Neuroscience 30:297–311.

Wictorin K, Clarke DJ, Bolam JP, Bjorklund A (1989): Host corticostriatal fibres establish synaptic connections with grafted striatal neurons in the ibotenic acid lesioned striatum. Eur J Neurosci 1:189–195.

Williams JT, Marshall KC (1987): Membrane properties and adrenergic responses in locus coeruleus neurons of young rats. J Neurosci 7:3687–3694.

Wilson CJ (1984): Passive cable properties of dendritic spines and spiny neurons. J Neurosci 41:281–297.

Wilson CJ (1992a): Dendritic morphology, inward rectification, and the functional properties of neostriatal neurons; in Single Neuron Computation Neural Nets: Foundations to Applications. New York, Academic Press, pp 141–171.

Wilson CJ (1992b): The generation of natural firing patterns in neostriatal neurons; in Arbuthnott GW, Emson PC (eds): Chemical Signalling in the Basal Ganglia. Prog Brain Res. Amsterdam, Elsevier, vol 99, pp 277–298.

Wilson CJ (1995): Corticostriatal neurons of the medial agranular cortex of rats; in Kimura M, Graybiel AM (eds): Functions of the Cortico-Basal Ganglia Loop. Tokyo, Springer, pp 50–72.

Wilson CJ, Chang HT, Kitai ST (1983a): Disfacilitation and long-lasting inhibition of neostriatal neurons in the rat. Exp Brain Res 51:227–235.

Wilson CJ, Chang HT, Kitai ST (1990a): Firing patterns and synaptic potentials of identified giant aspiny interneurons in the rat neostriatum. J Neurosci 10:508–519.

Wilson CJ, Groves PM (1980): Fine structure and synaptic connections of the common spiny neuron of the rat neostriatum: A study employing intracellular injection of horseradish peroxidase. J Comp Neurol 194:599–615.

Wilson CJ, Groves PM (1981): Spontaneous firing patterns of identified spiny neurons in the rat neostriatum. Brain Res 220:67–80.

Wilson CJ, Groves PM, Kitai ST, Linder JC (1983b): Three-dimensional structure of dendritic spines in the rat neostriatum. J Neurosci 3:383–398.

Wilson CJ, Kawaguchi Y (1996): The origins of two-state spontaneous membrane potential fluctuations of neostriatal spiny neurons. J Neurosci 16:2397–2410.

Wilson CJ, Xu ZC, Emson PC, Feler C (1990b): Anatomical and physiological properties of the cortical and thalamic innervations of neostriatal tissue grafts; in Dunnett SB, Richards S-J (eds): Progress in Brain Research. Amsterdam, Elsevier, vol 82, pp 417–426.

Xu ZC, Wilson CJ, Emson PC (1989): Restoration of the corticostriatal projection in rat neostriatal grafts: Electron microscopic analysis. Neuroscience 29:539–550.

Xu ZC, Wilson CJ, Emson PC (1991): Synaptic potentials evoked in spiny neurons in rat neostriatal grafts by cortical and thalamic stimulation. J Neurophysiol 65:477–493.

Xu ZC, Wilson CJ, Emson PC (1992): Morphology of intracellularly stained spiny neurons in rat striatal grafts. Neuroscience 48:95–110.

Zemanick MC, Walker PD, McAllister JP II (1987): Quantitative analysis of dendrites from transplanted neostriatal neurons. Brain Res 414:149–152.